Comparative Study of CZTS Thin Film Solar Cell with Different Buffer and Window Layer

by

Md. Noumil Tousif (122402)
A. A. Ferdous (122404)
Sakib Mohammad (122472)

A Thesis Submitted to the Academic Faculty in Partial Fulfillment of the Requirements for the Degree of

BACHELOR OF SCIENCE IN ELECTRICAL AND ELECTRONIC ENGINEERING

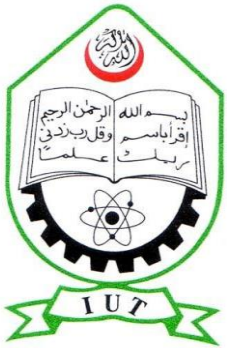

Department of Electrical and Electronic Engineering
Islamic University of Technology (IUT)
Gazipur, Bangladesh

November 2016

Declaration of Candidate

It is hereby declared that this thesis or any part of it has not been submitted elsewhere for the award of any Degree or Diploma.

Prof. Dr. Md. Ashraful Hoque
Supervisor, Professor and Head of the Department,
Department of Electrical and Electronic Engineering,
Islamic University of Technology (IUT),
Boardbazar, Gazipur-1704.
Date: ……

_____	_____	_____
Md. Noumil Tousif	**A. A. Ferdous**	**Sakib Mohammad**
Student No: 122402	Student No. 122404	Student No. 122472
Academic Year: 2015-2016	Academic Year: 2015-2016	Academic Year: 2015-2016
Date: …..	Date: …..	Date: …..

Table of Contents

List of Tables

List of Figures

List of Acronyms

FF	Fill Factor
Jsc	Short circuit current density
Voc	Open circuit Voltage of solar cell

Acknowledgements

We are grateful to our thesis supervisor, Dr. Md. Ashraful Hoque, for his continuous guidance and motivation in completing our thesis. His constant demand for making the work more and more elaborate finally resulted in satisfactory outcomes. We would like to thank Md. Wahidur Rahman, for providing us with SCAPS and necessary directions. We would also like to thank the students and teachers of Department of Electrical and Electronics Engineering, Islamic University of Technology, for their constant support and help.

Abstract

Energy conversion efficiency is a major issue for photovoltaic cells today. Researchers are

continuously trying to improve the efficiency level of photovoltaic devices by introducing new materials and advanced concepts. The target is to reach a high efficiency level within affordable cost, which will lead to a mass generation of electricity using photovoltaic devices.

The performance of CZTS solar cell using two different buffer layers was numerically simulated. We used CdS (Cadmium Sulfide) and In_2S_3 (Indium Sulfide) alternately as buffer layer. Performance was recorded for different thicknesses of CZTS absorber layer, different thicknesses of buffer layer and different values of acceptor density of CZTS. Best efficiency was 22.66% (with V_{OC}= 0.9114 V, J_{SC}= 28.68 mA/cm^2, FF=86.68%) which was obtained with CdS as buffer layer. The thickness of CZTS layer was 5 µm and the acceptor density was $2*10^{14}$ cm^{-3}. Varying the thickness of buffer layer does not have any significant effect on the performance of this solar cell. Our simulated model can be used for fabricating solar cells with higher efficiency.

Chapter 1- Introduction

1.1 Research Introduction

Photovoltaic (PV) is a solar electricity which uses semiconductor materials to convert sunlight directly into electricity. PV has enjoyed extraordinary growth during the last few
years. This growth can be attributed to some of the advantages solar cell enjoys, such as, low
operation cost, environment friendliness, high reliability, modularity, low construction cost
and few more.
A general classification of modern day solar cell is shown below:

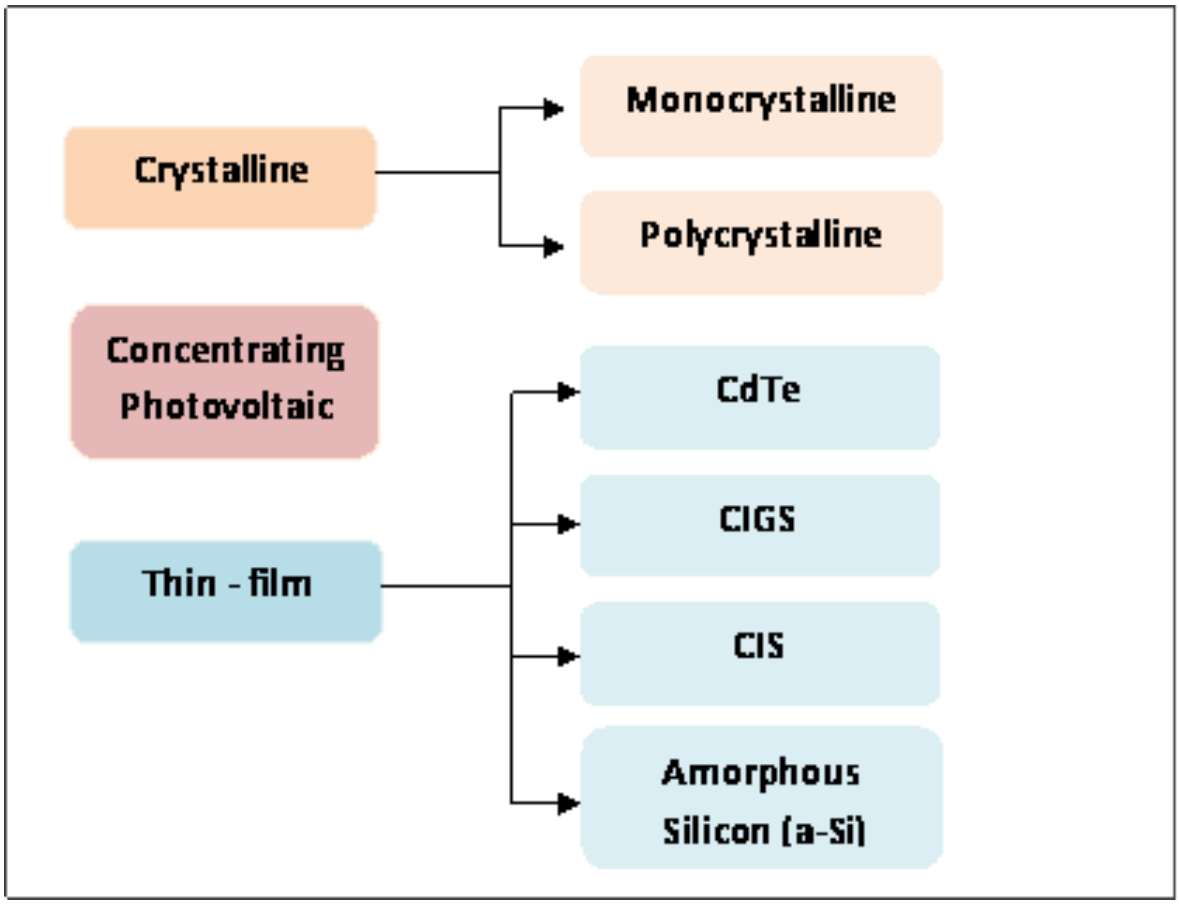

Fig. 1.1 General solar cell classification.

Thin film solar cell is gaining more focus in recent years due to obvious manufacturing cost issues. Particularly CZTS solar cell demands more attention than its counterparts because of

some unique advantages this solar cell possesses, namely, high efficiency, cost effectiveness, ability to be bulk produced and openness to wide fabrication procedures such as close-space sublimation (CSS), chemical vapor deposition (CVD), chemical bath deposition (CBD), and sputtering.

1.2 Research Motivation

Even though the materials like CIGS and CdTe appeared to be promising among the thin film solar cells with about 20% and 17% efficiencies respectively, the use of less abundant materials such as indium and gallium are hard to extract which make them not an ideal choice for large scale grid level production. Also, Cd which is extensively used in the manufacture of active material is a toxic heavy metal and can be an environmental hazard. The materials such as kesterite–structured copper zinc tin Chalcogenide (Cu2ZnSnS4/Se4) are recently considered as a potential replacement for CIGS and CdTe as they are made of earth abundant, inexpensive and non-toxic elements. Low band gap of the material ~1.0eV makes it a very good absorbent layer Few champion cells have been built already with efficiency of around 10.1%.
Another noteworthy point is that in all these cells CdS is used as buffer layer, which for the same reason as stated above is an environmental hazard and not recommended for use in large scale production which may lead to contamination of the area if not properly disposed. Even some countries are planning to pass legislation to regulate the use of toxic materials in PV cells. Due to these issues, it is preferable to avoid CdS as the buffer layer and use materials which are made of non-toxic elements. In this thesis, materials like ZnS, ZnSe and In_2S_3 are investigated as possible candidates for replacing the toxic CdS as the buffer layer. Although avoiding the use of CdS is a prime concern so, if it provides high efficiency we have to make a trade off.

1.3 Research Objective

This thesis proposes some modifications in the conventional CZTS solar cell to improve its efficiency and come as close as possible to the theoretical maximum efficiency of 30-33% for CZTS solar cells. CZTS solar cells have CZTS (p type semiconductor) as absorber or base layer and employ CdS or In_2S_3 (both n type semiconductor) as window layer. This p-n junction is
actually the core or building block of a solar cell. In practical, some other layers are necessary for functioning solar cell. Contact layers, window layer are some of these subsidiary
layers which also play crucial role in the functioning and stability of a solar cell.. The primary focus was on core layers, that is buffer and absorber layer to increase cell performance in terms of key output parameters such as efficiency, open circuit voltage (Voc), short circuit current density (Jsc) and fill factor (FF).

1.4 Research Outlines

In_2S_3 and CdS was alternatively used as buffer layer and separate simulations were done, for the window layer n type ZnO was chosen. For front and back contacts default settings was used that involved using flatbands for both contacts.

The temperature for the simulation was set constant at 300k and illumination was set as standard 1000 w/m^2 we have done simulations for ZnO/CdS/CZTS structure and ZnO/In_2S_3/CZTS separately. Although material defect is a notable concern however we neglected that for simplicity.
Our main concern was to choose a material for buffer layer that goes well with the CZTS layer. Besides other qualities it had to possess were cheapness, environmental safety and of course good abundance in earth's crust. Once these criteria were full filed we looked to optimize their thickness to obtain good output parameters.

Chapter 2- Background and Motivations

2.1 Solar Cell History

Solar cells are semiconductor devices which convert incident light into electricity by the absorption of photons and subsequent generation of electron-hole pairs. This effect of electricity generation from light absorption, which is known as the photovoltaic effect, was first observed by the French physicist A. E. Becquerel in 1839 [1]. The first solid-state photovoltaic cell was built many years later, by Charles Fritts, in 1883. He coated Selenium (Se) with an extremely thin layer of gold to form the junction. The photovoltaic device was less than 1% efficient [2]. The first practical photovoltaic cell was developed in 1954 at Bell Laboratories [3] by the three scientists- Daryl Chapin, Calvin Souther Fuller and Gerald Pearson. They used a diffused Silicon p-n junction that achieved 6% efficiency.
At present, solar cells are built with many different technologies, and the efficiency level that these devices can achieve is pretty good. In today‟s world, we have bulk Si solar cells, we have thin film solar cells fabricated from Si or CdTe, we have dye-sensitized solar cells, and so on. There are even more advanced concept solar cells like Quantum Dot (QD) solar cells, hot carrier solar cells etc. Today, solar cells are used for mass generation of electricity. The added advantage of solar power plants is that they require minimum maintenance, and the input energy is clean and free.

2.1.1 Principle of Operation

Figure 2.1 presents a simplified diagram [4] of a solar cell that utilizes a single p-n junction. With no voltage applied to this junction, an electric field exists in the depletion region of the p-n junction. A simple diagram shows the p-n junction at work which is the fundamental concept of a solar cell.

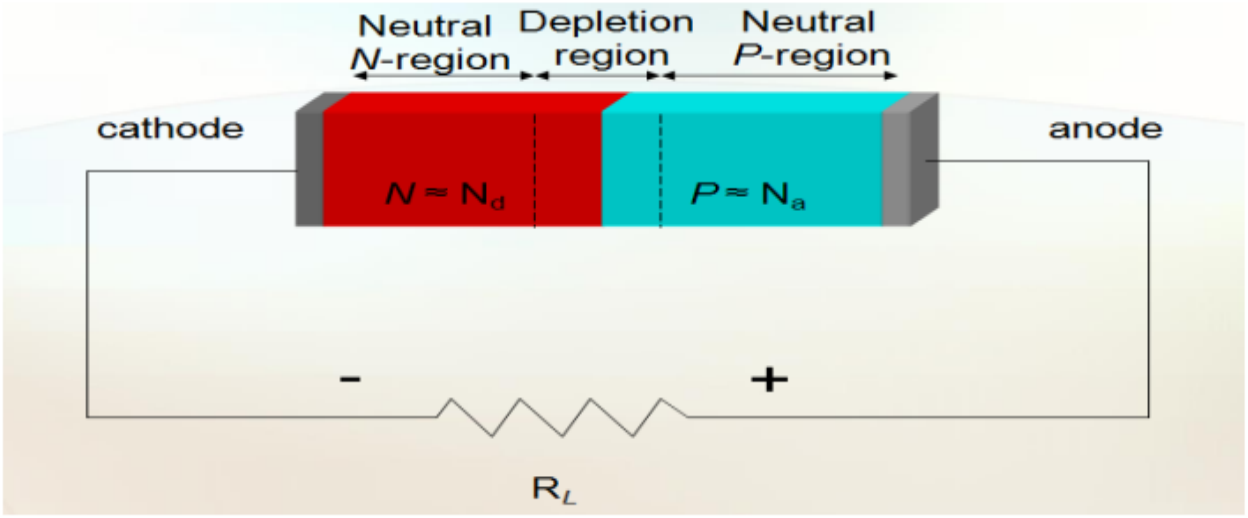

Fig. 2.1 Operation of a p-n junction

For simplicity, we consider that a resistive load is connected with the device. Now, photons incident on the device can create electron-hole pairs in the space-charge region, which are forcibly swept out of the depletion region by the built-in electric field, as the depletion region must be depleted of free charges. This swept out carriers produce a photocurrent I_L, in the reverse-bias direction for the p-n junction. Now, the photocurrent I_L produces a voltage drop across the resistive load, which forward biases the p-n junction. This forward bias produces a forward current, I_F, in the forward-bias direction for the p-n junction. The net current, I, in the reverse bias direction for the p-n junction, is given by equation (1). Fig. 2.2 shows a simplified schematic diagram of a solar cell.

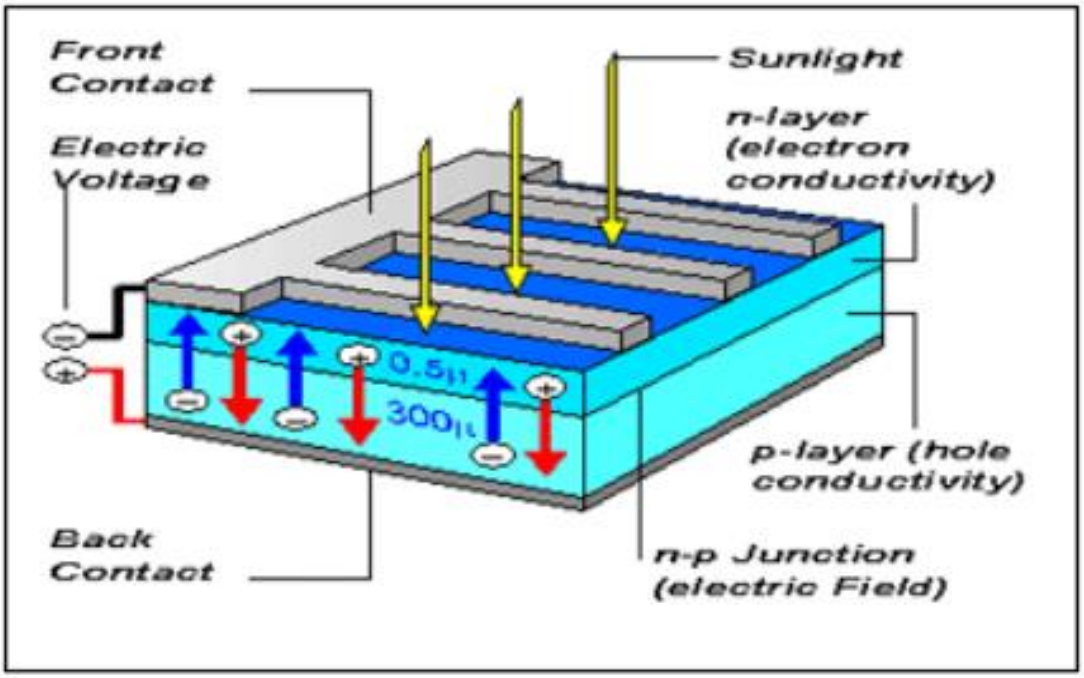

Fig. 2.2 Schematic diagram of a simplified back contact solar cell (image courtesy: ECN, the Netherlands)

$I = I_L - I_F = I_L - I_S\,[exp\,(qV / nkT) - 1]$ (1)

Where,

n = Ideality factor (taken as 1)

k= Boltzmann constant

T= Temperature in K

q = charge of an electron

I_S = saturation current

2.1.2 Important Quantities

Now, there are two quantities of practical interest, the short-circuit current (I_{sc}) and the open circuit voltage (V_{oc}). The short-circuit condition occurs when the resistive load is zero, so that V= 0. In this case, I_F is zero, and the short-circuit current, I_{sc}, is given by equation (2).

$I_{sc} = I_L$ (2)

Open-circuit condition occurs when the load resistance is infinity. The net current is zero in this case, which finally gives the expression of the open-circuit voltage, V_{oc}, as shown in equation (3).

$V_{oc} = (nkT / q)\,ln\,(1 + (I_L / I_S))$ (3)

It is to be noted that at both short-circuit and open-circuit condition, the power output of a solar cell is zero. Actually, there is a maximum power point on the I-V characteristics graph of a solar cell where $\frac{dp}{dv}$ =0 (P is the output power). This point is called the maximum power point. The maximum output power, P_m, is given by,

$P_m = V_m I_m$ (4)

Where,

V_m = Voltage at Maximum Power Point

I_m = Current at Maximum Power Point

Now, a quantity, termed as „Fill Factor", is used to measure the "squareness" of the I-V curve of a solar cell. This is the ratio of the maximum output power, P_m, to the product of short-circuit current (I_{sc}) and the open-circuit voltage (V_{oc}). Fill factor is commonly abbreviated as FF. A higher FF is desirable, since it increases the maximum output power. The theoretical FF from a solar cell can be determined by differentiating the power from a solar cell with respect to the voltage and finding the voltage value for which the derivative equals to zero. This is the voltage corresponding to the maximum power point, which is denoted by V_m. An equation involving V_m is given in (5).

$V_m = V_{oc} - [(nkT / q) \times [ln(qV_m / nkT) + 1]$ (5)

Solving equation (5) by iteration gives the value of V_m. Now, determining the value of I_m requires the knowledge of I_L and I_S. So, this method does not give a closed form solution for determining the maximum output power P_m, the knowledge of which is required for determining FF. So, for all the simulations in our work, we have used the formula (5) given by equation (6) for the calculation of FF.

$$FF = \frac{Vocn - \ln(Vocn + 0.72)}{Vocn + 1} \quad (6)$$

Where,

$$Vocn = \left(\frac{q}{nkt}\right) Voc \quad (7)$$

Here,

V_{oc}= Open-circuit voltage (in Volt)

n = Ideality factor

q= Charge of an electron = 1.6×10^{-19} Coulomb

k= Boltzmann constant

T= Temperature in K

For all the simulations, we have considered n=1, and T = 300K.

The energy conversion efficiency of a solar cell, η, is given in (8).

$$\eta = \frac{Voc * Isc * FF}{E * A} * 100\% \quad (8)$$

Here,

V_{oc}= Open-circuit voltage (in Volts)

I_{sc}= Short-circuit current (in Amperes)

FF= Fill Factor

E= Solar irradiance (in W/cm^2)

A= Area of the solar cell (in cm^2)

Now, I_{sc}/A can be termed as J_{sc}, which is the short-circuit current density (in A/cm^2). So, equation (8) can be rewritten as,

$$\eta = \frac{Voc * Isc * FF}{E} * 100\% \quad (9)$$

Where,

J_{sc}= Short-circuit current density (in A/cm^2)

We are considering the use of the solar cell for terrestrial applications. So, to account for the incident sunlight, AM1.5G illumination was considered in the simulation code, as this is the standard terrestrial illumination. According to this, the solar irradiance, E, is taken to be 1000 W/m^2, or, 0.1 W/cm^2. It was also considered that the device is working under 1 sun i.e. no concentrator is used. Using Equation (9), the energy conversion efficiency was calculated.

2.2 Heterojunction Solar Cells

A heterojunction is a p-n junction formed between two different semiconducting materials. Heterojunctions have got numerous applications in optoelectronic devices [6]. Heterojunction solar cells generally employ a p-n or p-i-n structure. In the simplified p-n structure, one material essentially works as an absorber, while the other can be a window layer, or another absorber [7]. The absorber is the functioning layer for optical absorption and generation of electron-hole pairs. The window layer is usually a high bandgap material which is highly transparent to light, so that it can allow almost all the incident photons to reach the absorber. Heterojunction devices have an inherent advantage over homojunction devices, which require materials that can be doped both p- and n-type. Many semiconducting materials can be doped either p-type or n-type, but not the both. Heterojunctions do not suffer from this limitation. So, many promising materials with good optical absorption capabilities can be investigated to

produce optimal cells [8]. Again, a high-bandgap window layer reduces the cell's series resistance, and improves the output voltage [8]. It also helps to reduce recombination of minority carriers at the metal semiconductor interface around the contacts [9].
For solar cells and other optoelectronic components, it is not sufficient to choose materials with suitable bandgap values and bring them to form a junction. It is also important to make sure that the chosen materials form a junction such that the interface is as freer of energy states in the forbidden band as possible, in order to prevent additional recombination of carriers and carrier trapping [9]. Material combinations satisfying such conditions are not very common. However, many combinations of III-V and II-VI compounds, especially the ternary compounds, satisfy these criteria to large extents [9].

2.3 Silicon Alloys or II-VI Materials – which one is a better choice for Heterojunctions?

Heterojunction solar cells involving Si and Si alloys have been thoroughly investigated [10]. But from a fundamental standpoint, Si is not a very good choice. Its bandgap is lower than the optimum bandgap required for achieving the highest level of efficiency. For terrestrial applications, the optimum bandgap of the absorber should be around 1.4 eV [11], while Si has an indirect bandgap of 1.12 eV. Besides this, Si has low optical absorption coefficient, compared to the high optical-absorption-compounds [12].
Now-a-days, II-VI compounds have gained considerable interest as constituents of both single-junction and multijunction solar cells. The special advantage that these materials offer is their wide range of variation in bandgaps. Besides this, they have got high optical absorption properties, along with high electron mobility and high minority carrier lifetime. They also provide numerous options for proper lattice matching between the heterojunction materials. So, photovoltaic cells fabricated from II-VI compounds typically provide high output current and high efficiency. II-VI ternary and quaternary alloys can offer yet more flexibility, as their bandgaps and other properties can be finely tuned by changing the alloy composition.

2.4 CZTS Solar Cell

Even though the materials like CIGS and CdTe appeared to be promising among the thin film solar cells with about 20% and 17% efficiencies respectively, the use of less abundant materials such as indium and gallium are hard to extract which make them not an ideal choice for large scale grid level production. Also, Cd which is extensively used in the manufacture of active material is a toxic heavy metal and can be an environmental hazard. The materials such as kesterite–structured copper zinc tin Chalcogenide (Cu2ZnSnS4/Se4) are recently considered as a potential replacement for CIGS and CdTe as they are made of earth abundant, inexpensive and non-toxic elements. Low band gap of the material ~1.0eV makes it a very good absorbent layer few champion cells have been built already with efficiency of around 10.1%.
Another noteworthy point is that in all these cells CdS is used as buffer layer, which for the same reason as stated above is an environmental hazard and not recommended for use in large scale production which may lead to contamination of the area if not properly disposed. Even some countries are planning to pass legislation to regulate the use of toxic materials in PV cells. Due to these issues, it is preferable to avoid CdS as the buffer layer and use

materials which are made of non-toxic elements. In this thesis, materials like ZnS, ZnSe and In3S3 are investigated as possible candidates for replacing the toxic CdS as the buffer layer. In the following sections, an optical model that is developed to calculate the external quantum efficiency (EQE), short circuit current density and other optical responses is discussed briefly

2.5 Drawback of II-VI Solar Cells

The problem associated with II-VI solar cells is that these cells are very expensive, compared to the commonly used terrestrial solar cell technologies [37]. This is mainly due to the high fabrication cost of II-VI materials, along with the unavailability of necessary fabrication technology in few cases. So, the use of II-VI solar cells is still limited to applications, where the efficiency is prioritized over the cost [38, 39]. Utilization of such solar cells for general terrestrial applications requires reduction of materials processing and fabrication costs. Another way to address this problem is to use concentrators with solar cells. Concentrated solar cells can give up to 2000 times the power output of a solar cell working under 1 sun, depending on the concentration level. Though concentrators are very expensive, they can offer a good trade-off between the PV system cost and the achievable high efficiency [40-42].

2.6 About the Software

SCAPS is a one dimensional solar cell simulation program developed at the department of Electronics and
Information Systems (ELIS) of the University of Gent, Belgium.
SCAPS is originally developed for cell structures of the CuInSe2 and the CdTe family. Several extensions
however have improved its capabilities so that it is also applicable to crystalline solar cells (Si and GaAs
family) and amorphous cells (a-Si and micromorphous Si). An overview of its main features is given below:

- up to 7 semiconductor layers
- almost all parameters can be graded (i.e. dependent on the ocal composition or on the depth in the cell):

$Eg, \chi, \varepsilon, N_C, N_V, v_{thn}, v_{thp}, \mu_n, \mu_p, N_A, N_D,$ all traps (defects) N_t

- recombination mechanisms: band-to-band (direct), Auger, SRH-type
- defect levels: in bulk or at interface; their charge state and recombination is accounted for
- defect levels, charge type: no charge (idealization), monovalent (single donor, acceptor), divalent (double
donor, double acceptor, amphoteric), multivalent (user defined)
- defect levels, energetic distributions: single level, uniform, Gauss, tail, or combinations
- defect levels, optical property: direct excitation with light possible (impurity photovoltaic effect, IPV)
- defect levels, metastable transitions between defects
- contacts: work function or flat-band; optical property (reflection of transmission filter) filter
- tunneling: intra-band tunneling (within a conduction band or within a valence band);

tunneling to and
from interface states
• generation: either from internal calculation or from user supplied $g(x)$ file
• illumination: a variety of standard and other spectra included (AM0, AM1.5D, AM1.5G, AM1.5Gedition2, monochromatic, white,...)
The startup panel of SCAPS is shown below

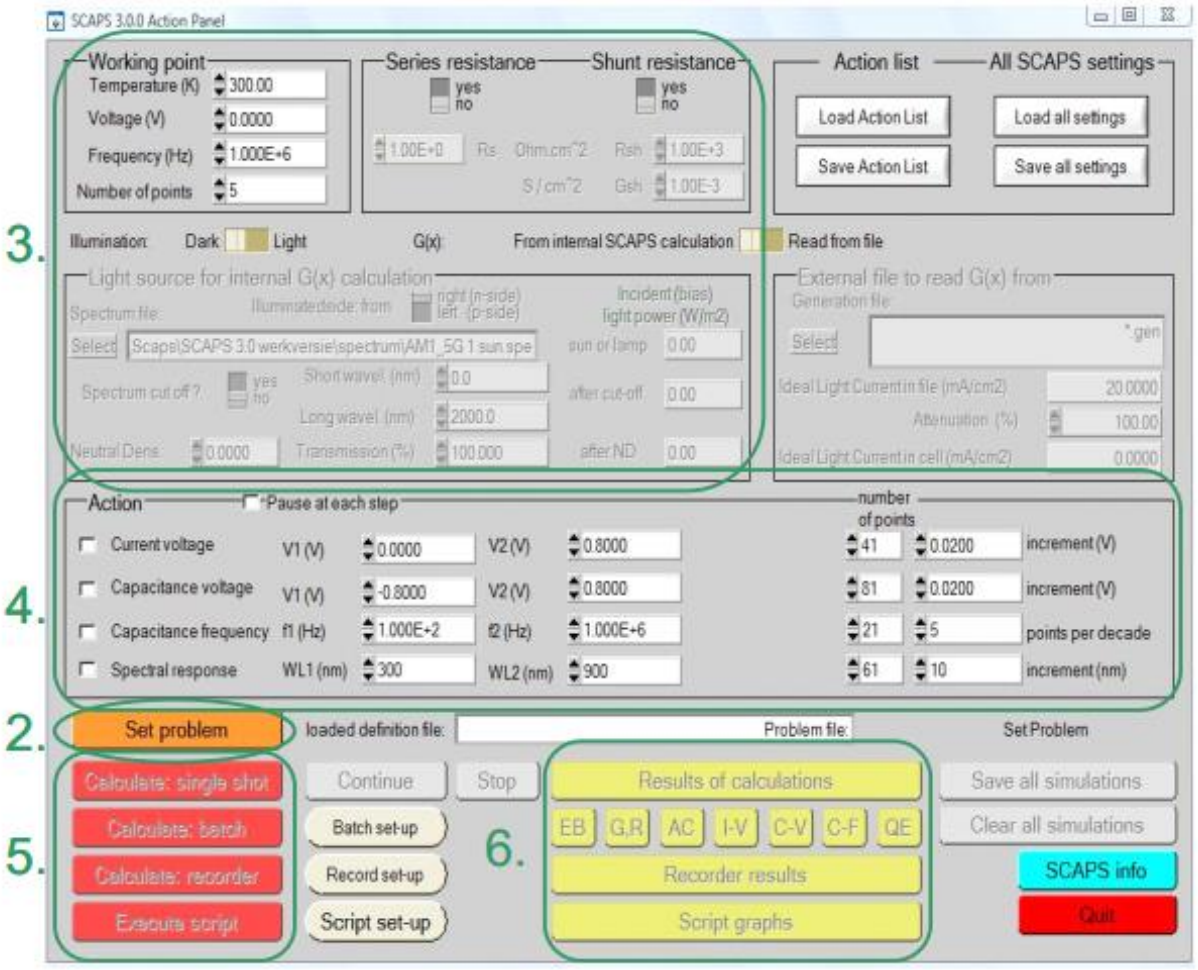

Figure 2.1 The SCAPS start-up panel: the Action panel or main panel. The meaning of the blocks numbered 1 to 6 is
explained in the text.

There are dedicated panels for the basic actions:
1. Run SCAPS .
2. Define the problem, thus the geometry, the materials, all properties of your solar cell
3. Indicate the circumstances in which you want to do the simulation, i.e. specify the working point
4. Indicate what you will calculate, i.e. which measurement you will simulate.
5. Start the calculation(s)
6. Display the simulated curves

Chapter 3- Methodology

3.1 Selecting Initial Design

In order to demonstrate the drawbacks of conventional CZTS solar cell an initial design was chosen which will serve as foundation for the modified structure to be proposed later on. The initial design consists of six layers namely; Transparent Conductive Oxide (TCO/ CTO), a buffer layer, a window layer, an absorber laye. For the initial design Tin Oxide (SnO_2) was chosen as TCO, Zinc Oxide (ZnO) was chosen as buffer layer, CdS as window layer, CdTe as absorber and Cu_2Te as BSR. This initial structure of Ni/Al, Ni, Al, Ag, AZO as front contact, , i Zno/Al:ZnO, ITO as Window layer, CdS, ZnS, ZnSe, In2S3, CdS/In2S3 as Buffer layer, CZTS as Absorber layer, Mo, Ni as Back contact and SLG as substrate shall be the starting point of this thesis.

The schematic structure of the initial design is shown in Fig. 3.1.

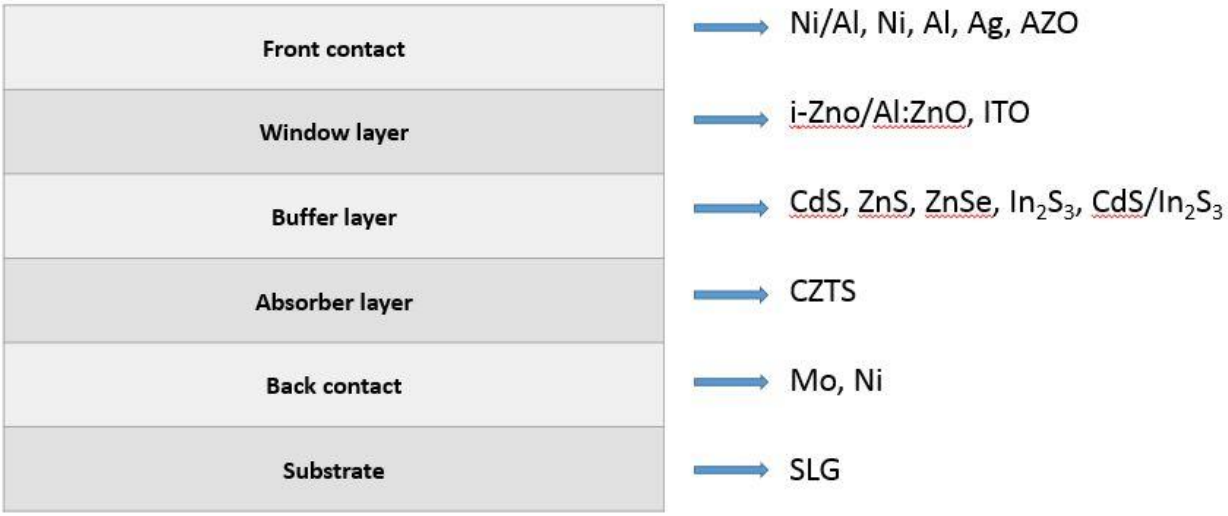

Fig. 3.1 Schematic diagram of the initial CZTS solar cell.

3.1.1 Choice of Layer Materials

For the purpose of simulation in SCAPS 3302, some key parameters of the layers were to be keyed in. These parameters are to remain unchanged for the future design and simulations unless otherwise specified. Table 3.1 shows the general layer parameters.

Table 3.1

General layer parameters

	n-ZnO	**n-CdS**	**n-In_2S_3**	**p-CZTS**
Layer thickness (µm)	0.2	0.05	0.05	5
Di-electric permittivity (relative)	9	9	13.5	10
Electron mobility (cm2/Vs)	100	350	400	100
Hole mobility (cm2/Vs)	25	5	210	2.5
NA (Shallow uniform acceptor density) (1/cm3)	0	0	1	$2*10^{14}$
ND (Shallow uniform donor density) (1/cm3)	$1*10^{18}$	$1*10^{17}$	$1*10^{18}$	1
Band Gap (eV)	3.3	2.41	2.8	1.5
Nc (CB effective density of states) (1/cm3)	$2.2*10^{18}$	$1.8*10^{19}$	$1.8*10^{19}$	$2.2*10^{18}$
Nv (VB effective density of states) (1/cm3)	$1.8*10^{19}$	$2.4*10^{18}$	$4*10^{13}$	$1.8*10^{19}$
Electron affinity (eV)	4.6	4.5	4.7	4.5

3.1.2 Choice of Contact Materials

Nickel (Ni) was chosen as contacts because of its superior performance recently observed as contact layer material.Table 3.2 list the contact parameters used in AMPS 1D for the simulation purpose and will remain unchanged throughout the study for several other simulations to come

Table 3.2

Contact parameters

Parameters	Front contact	Back contact
Φ_b [eV]	$\Phi_{bn} = 0.10$	$\Phi_{bp} = 1.25$
S_e [cm/s]	1×10^7	1×10^7
S_h [cm/s]	1×10^7	1×10^7
R_f [I]	0.01	0.99

Where,

S_e = Surface electron velocity (cm/s)

S_h = Surface hole velocity (cm/s)

R_f = Reflectibilty (0~1)

Φ_b = Barrier hieght (eV)

3.2 First Modified Structure

The first modified structure involves replacing conventional window layer CdS with tertiary compound CdZnS whose band gap along with other characteristics are changeable between its two binary constituents CdS and ZnS by changing the alloy composition in $Cd_xZn_{1-x}S$. The objective is to attain a larger bandgap than existing 2.42 eV to allow photons of maximum possible wavelength through.

3.2.1 Layer Parameters for the First Modified Structure

At the beginning, some default values of contact parameters and general layer parameters for each layer of the device was chosen that are listed in Table 3.3 and 3.4 respectively.

Table 3.3

Contact parameters

Parameters	Front contact	Back contact
Φ_b [eV]	$\Phi_{bn} = 0.10$	$\Phi_{bp} = 1.25$
S_e [cm/s]	1×10^{7}	1×10^{7}
S_h [cm/s]	1×10^{7}	1×10^{7}
R_f [I]	0.01	0.99

Table 3.4

General layer parameters

	n-ZnO	**n-CdS**	**p-CZTS**
Layer thickness (μm)	0.2	0.05	5
Di-electric permittivity (relative)	9	9	10
Electron mobility (cm2/Vs)	100	350	100
Hole mobility (cm2/Vs)	25	5	2.5
NA (Shallow uniform acceptor density) (1/cm3)	0	0	$2*10^{14}$
ND (Shallow uniform donor density) (1/cm3)	$1*10^{18}$	$1*10^{17}$	1
Band Gap (eV)	3.3	2.41	1.5
Nc (CB effective density of states) (1/cm3)	$2.2*10^{18}$	$1.8*10^{19}$	$2.2*10^{18}$
Nv (VB effective density of states) (1/cm3)	$1.8*10^{19}$	$2.4*10^{18}$	$1.8*10^{19}$
Electron affinity (eV)	4.6	4.5	4.5

3.2.2 Modelling the Window Layer for the First Modified Structure

In this part of the work, a new window layer material, $Cd_{1-x}Zn_xS$ was introduced that replaced the CdS in the initial design. Next, keeping every other device parameter fixed at some default (initial) value, simulations were run for different value of x (e.g. x=0, 0.2, 0.4, 0.6, 0.8 and 1) and changes in the output characteristics were observed. $Cd_{1-x}Zn_xS$ is ternary II-VI compound comprised of two binary compound CdS and ZnS. So by changing the value of x, each time we get a material that is precise mixture of CdS (for x=0) and ZnS (for x=1). Simulation was conducted with these default values, and a light J-V characteristics graph was acquired.
From the graph, values of open-circuit voltage (V_{oc}), short-circuit current density (J_{sc}), Fill factor (FF) and efficiency (η) were obtained. FF and efficiency can also be calculated using the equations (6) and (9), respectively.
This efficiency is the efficiency under standard conditions. First batch of simulations was run for $Cd_{1-x}Zn_xS$/CdTe where only window layer was modified by changing Zn concentration x% and all other layers with all their baseline parameters were kept unchanged. Simulations were run for x=0, 0.2, 0.4, 0.6, 0.8, 1. 20 The objective was to find out and analyse the effect of molar composition in $Cd_{1-x}Zn_xS$ on $Cd_{1-x}Zn_xS$/CdTe solar cell. Changing value of x each time meant having a totally different material altogether with its unique electrical and optical parameters. So six sets of simulations were run for six values of x (x=0, 0.2, 0.4, 0.6, 0.8, 1) keeping all other layer parameters unchanged with careful modification only for window layer, $Cd_{1-x}Zn_xS$ according to different values for x

3.3 Second modified structure

Secondly, conventional absorber layer CZTS was replaced with another ternary compound $Cd_xZn_{1-x}Te$ to utilize variation in different parameter‟s value by changing alloy composition with an optimal value of x in $Cd_xZn_{1-x}S$ found from first modified structure simulations. This time the objective was to improve the existing poor lattice mismatch (almost 10%) between window and absorber layer.

3.3.1 Layer parameters for the second modified structure

Before conducting simulations, some default values for thickness, doping concentration and alloy composition for each layer were fixed. Table 3.5 and 3.6 summarizes these default values

Table 3.5

Contact parameters

Parameters	Front contact	Back contact
Φ_b [eV]	$\Phi_{bn} = 0.10$	$\Phi_{bp} = 1.25$
S_e [cm/s]	1×10^7	1×10^7
S_h [cm/s]	1×10^7	1×10^7
R_f [I]	0.01	0.99

Layer thickness (μm)	0.2	0.05	5
Di-electric permittivity (relative)	9	9	10
Electron mobility (cm2/Vs)	100	350	100
Hole mobility (cm2/Vs)	25	5	2.5
NA (Shallow uniform acceptor density) (1/cm3)	0	0	$2*10^{14}$
ND (Shallow uniform donor density) (1/cm3)	$1*10^{18}$	$1*10^{17}$	1

Band Gap (eV)	3.3	2.41	1.5
Nc (CB effective density of states) (1/cm3)	$2.2*10^{18}$	$1.8*10^{19}$	$2.2*10^{18}$
Nv (VB effective density of states) (1/cm3)	$1.8*10^{19}$	$2.4*10^{18}$	$1.8*10^{19}$
Electron affinity (eV)	4.6	4.5	4.5

3.3.2 Modelling the absorber layer for the second modified structure

In the previous section we discussed about a modified window layer introduced in our initial design to replace original window layer of CdS to improve the bandgap and thus increase carrier current. After the successful completion of that task it is the second drawback of conventional CZTS solar cell that this section aims to encounter. For that purpose, keeping the modified window layer ($Cd_{1-x}Zn_xS$) with the best result (e.g x=0.2) obtained from previous section, a new absorber layer was introduced and analysed in this section. Another ternary compound CZTS replaced original CZTSSe as the absorber layer to minimize the lattice mismatch between window and absorber layer that was prevalent in the conventional design. The second batch of simulations conducted in this section was run for $Cd_{0.8}Zn_{0.2}S/Cd_{1-x}Zn_xTe$. The study was to investigate the effect of varying alloy composition in $Cd_{1-x}Zn_xTe$on a particular modified $Cd_{1-x}Zn_xS$ (here x=0.2) window layer with improved bandgap and Jsc. The idea was to observe whether improving the lattice matching by varying Zn concentration x% of $Cd_{1-x}Zn_xTe$ can improve the efficiency of the cell with a modified window layer. Now, simulations were conducted by varying the value of x for the absorber layer alloy ($Cd_{1-x}Zn_xTe$) from 0 to 1, in steps of 0.2. For each simulation, value of every other device parameter was kept the same as listed in Table 3.5 and 3.6. Now, a light J-V characteristics curve was obtained for every simulation, which provided the energy conversion efficiency, Jsc, Voc and FF for that particular simulation. In this manner, efficiency, Jsc, Voc and FF for each of the simulations was obtained. Then, these output parameters were plotted against x (Zinc mole fraction) for the absorber layer. The efficiency curve, Jsccurve, Voc curve and FF curve were analysed for getting an idea about the optimization of Zinc mole fraction in $Cd_{1-x}Zn_xTe$ for achieving higher efficiency. Afterwards, through analysing the output parameters with varying x value, an optimum absorber layer was found. Together with the optimum window layer achieved in the last section, section 3.4 discusses the optimum solar cell design this thesis proposes and further aims to analyse the proposed structure against other design variables.

3.4 Optimized structure

From article 3.2 and 3.3 a new solar structure was developed by modifying the window and absorber layer in the initial design of TCO/ZnO/CdS/CZTS/Ni. Schematic diagram of the new cell is shown in figure 3.2. In this chapter the proposed solar cell will be investigated against some typical input design parameters such as window thickness, absorber thickness and temperature to further analyse this new design in order to improve its performance in terms of efficiency and stability.

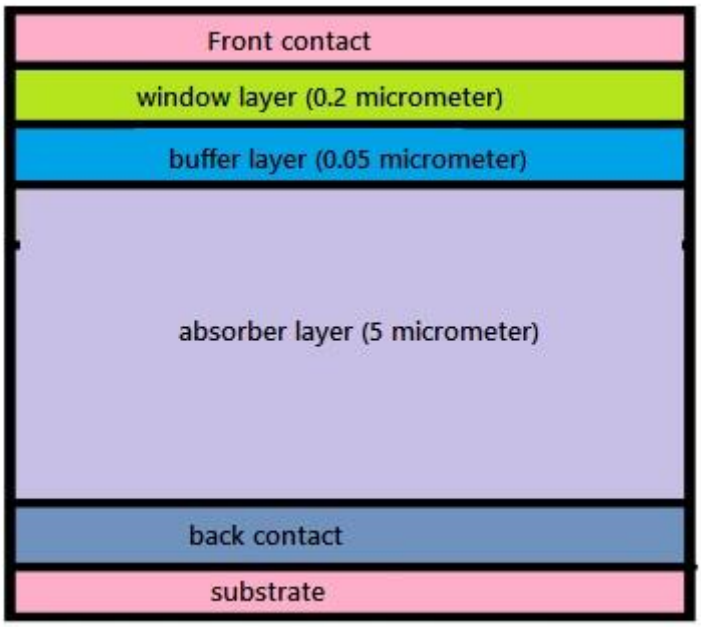

Fig. 3.2 Schematic diagram of the proposed solar cell

Chapter 4- Results and Discussions

4.1 The Initial Design

The different results and effects along with discussions of the initial design simulations are presented in the following sections. As already mentioned earlier, the initial design is made of Ni/Al, Ni, Al, Ag, AZO as front contact, , i Zno/Al:ZnO, ITO as Window layer, CdS, ZnS, ZnSe, In2S3, CdS/In2S3 as Buffer layer, CZTS as Absorber layer, Mo, Ni as Back contact and SLG.

4.1.1 J-V curve with CdS as buffer layer

Figure 4.1 shows that the initial design yields an open-circuit voltage (V_{oc}) of -0.9114 V, and the short-circuit current density (J_{sc}) is 28.68 mA/cm2. For this simulation, the fill factor was found to be 86.68%. This design is already resulting in high efficiency of 22.66% because of advanced layer designs. The introduction of high quality TCO along with buffer layer make this design a very improved one.

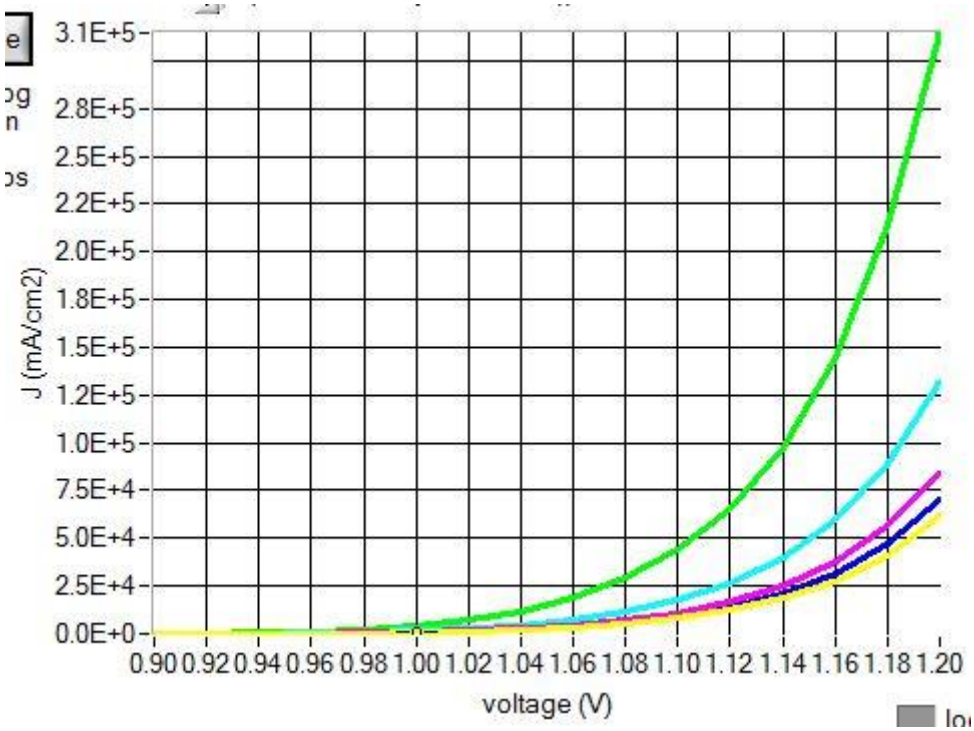

Fig. 4.1 J-V curve of solar cell using CdS buffer layer

4.1.2 J-V curve with In_2S_3 as buffer layer

Figure 4.1 shows that the initial design yields an open-circuit voltage (V_{oc}) of -0.9114 V, and the short-circuit current density (J_{sc}) is 28.68 mA/cm2. For this simulation, the fill factor was found to be 86.68%. This design is already resulting in high efficiency of 22.66% because of advanced layer designs. The introduction of high quality TCO along with buffer layer make this design a very improved one.

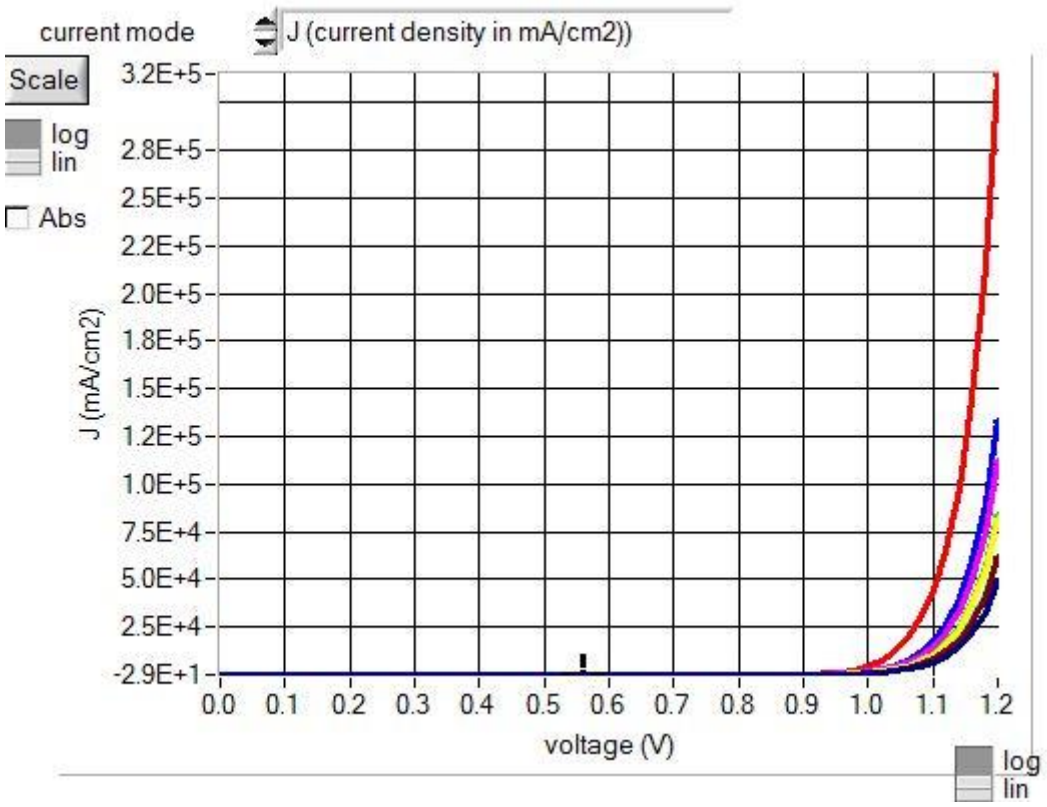

Fig 4.2 Fig. 4.1 J-V curve of solar cell using In_2S_3 buffer layer

4.2.1 Spectral response with CdS as buffer layer

Figure 4.1 shows that the initial design yields an open-circuit voltage (V_{oc}) of -0.9114 V, and the short-circuit current density (J_{sc}) is 28.68 mA/cm$_2$. For this simulation, the fill factor was found to be 86.68%. This design is already resulting in high efficiency of 22.66% because of advanced layer designs. The introduction of high quality TCO along with buffer layer make this design a very improved one.

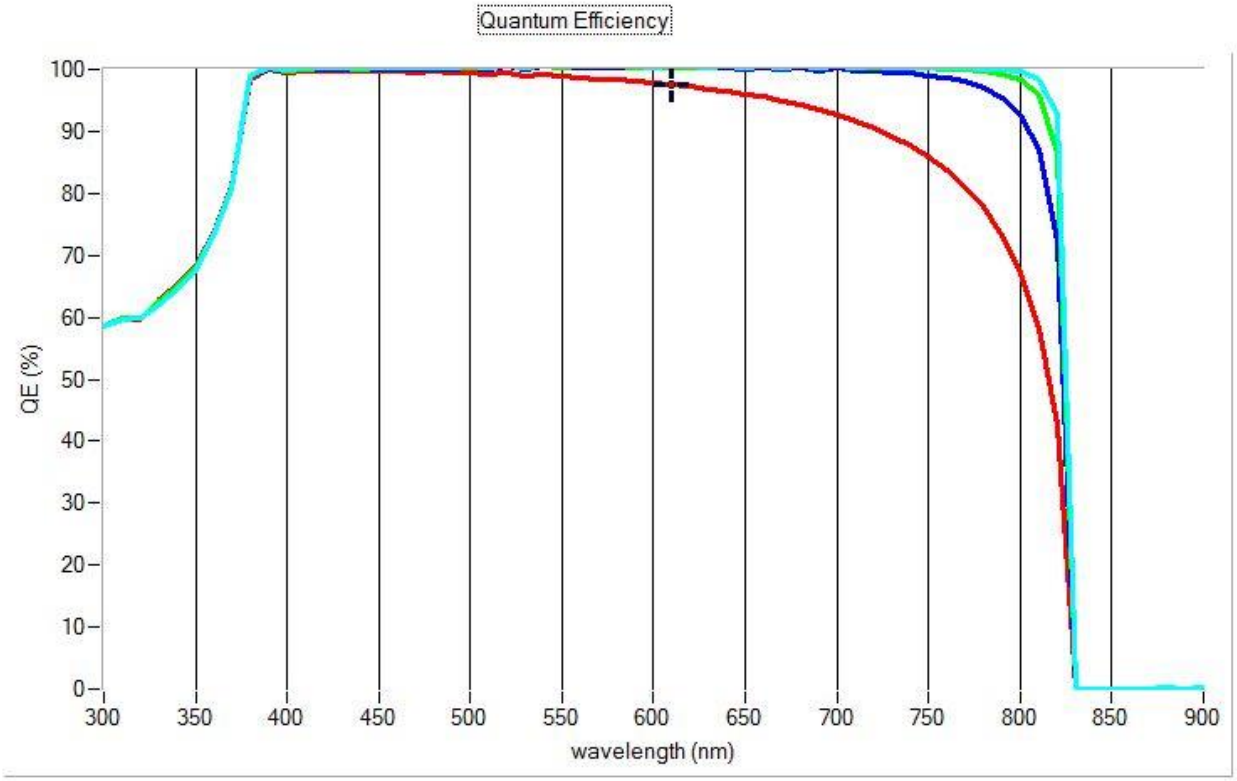

Fig 4.3 spectral response of solar cell with CdS buffer layer

4.2.2 Spectral response with In_2S_3 as buffer layer

Figure 4.4 shows that the initial design yields an open-circuit voltage (V_{oc}) of -0.9114 V, and the short-circuit current density (J_{sc}) is 28.68 mA/cm_2. For this simulation, the fill factor was found to be 86.68%. This design is already resulting in high efficiency of 22.66% because of advanced layer designs. The introduction of high quality TCO along with buffer layer make this design a very improved one.

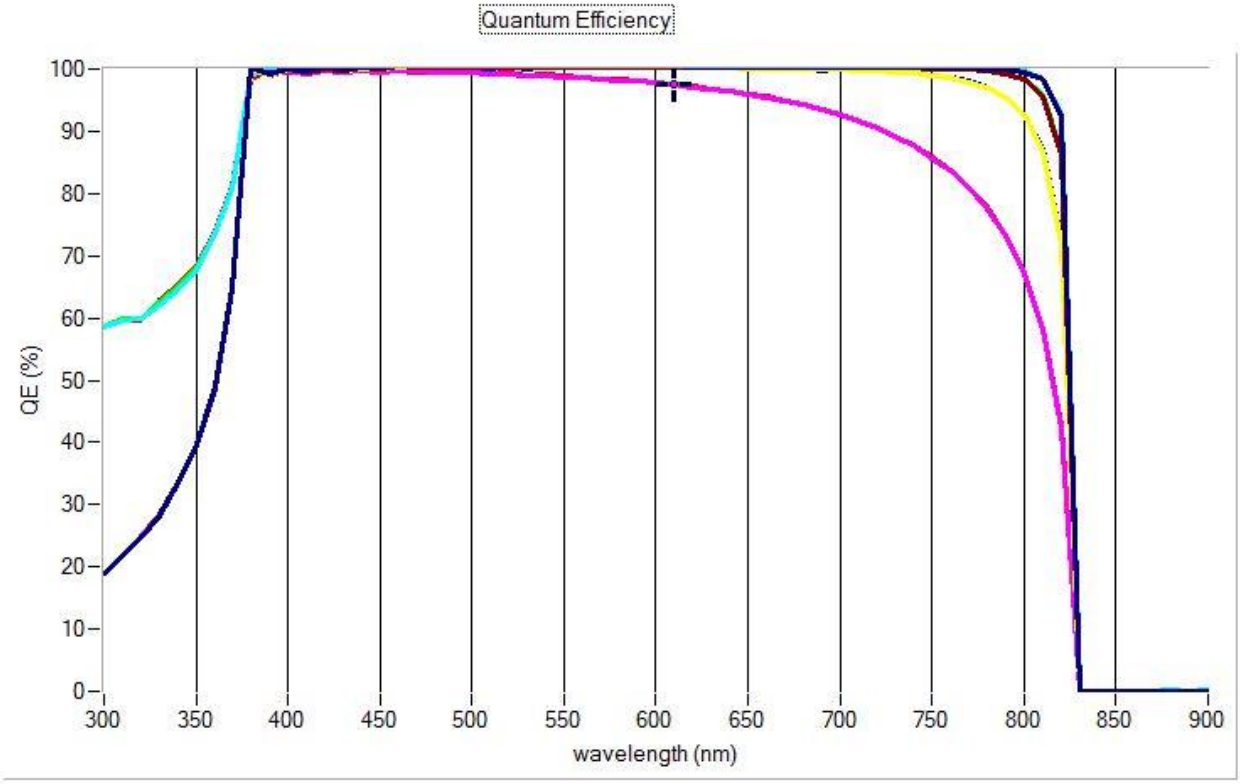

Fig 4.4 spectral response of solar cell with In_2S_3 buffer layer

4.3 Effect of resistance

Resistances present in the circuit plays some role in determining the performance of the solar cell.

4.3.1 Resistance vs efficiency

In Fig 4.5, we can see that the efficiency decreases almost linearly with increasing values of resistances.

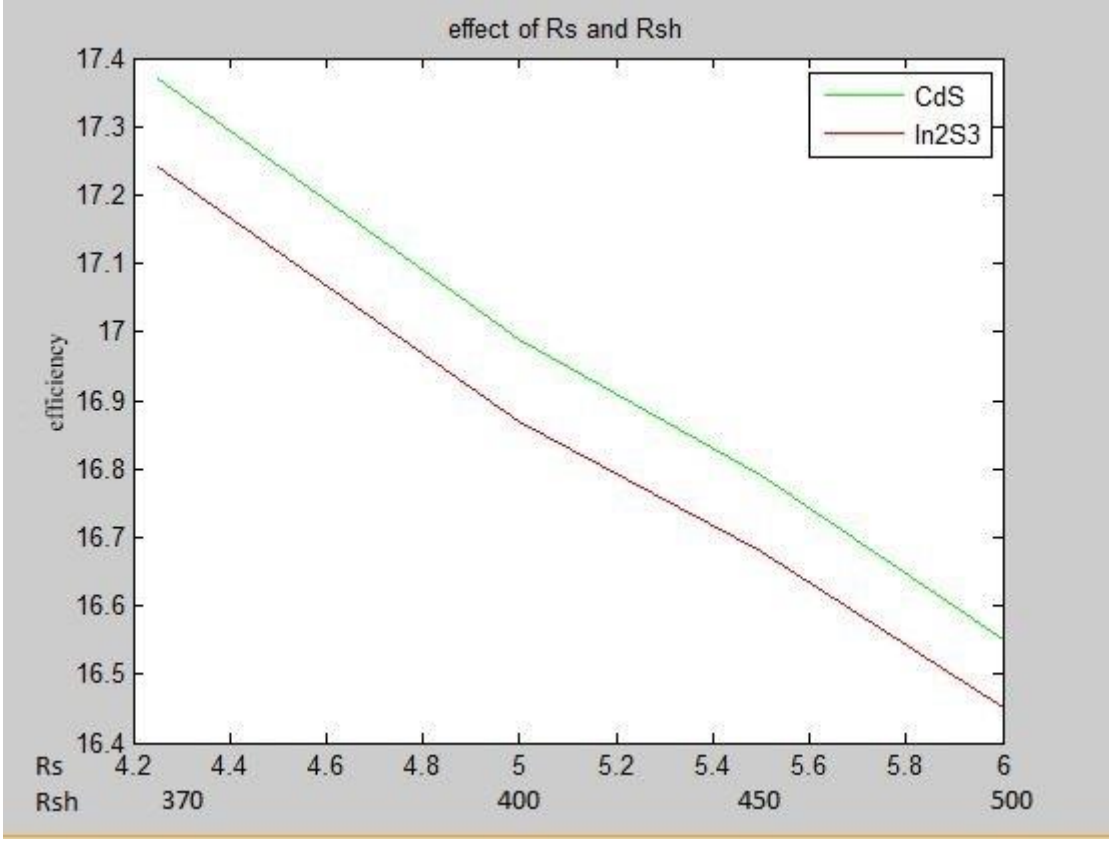

Fig 4.5 effect of resistances on efficiency of solar cell

4.3.2 Resistance vs FF

Fig 4.6, effect of resistance on Fill Factor is shown.

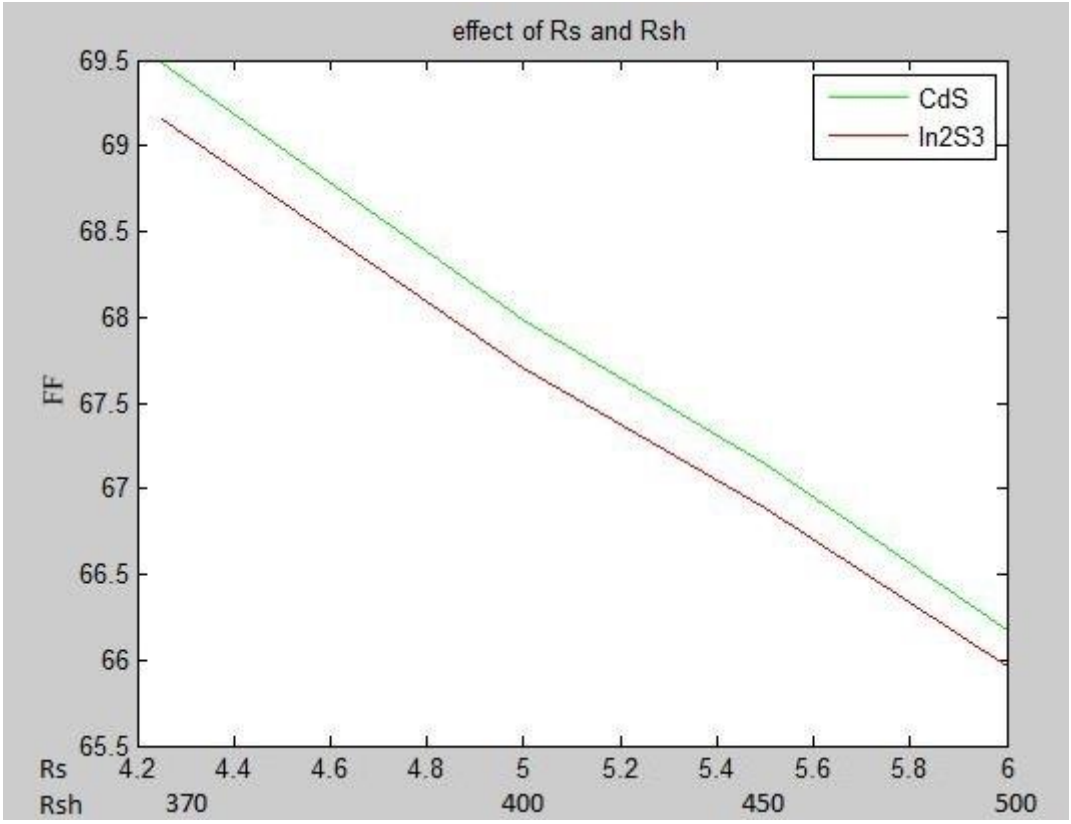

Fig 4.6 effect of resistances on FF of solar cell

4.3.3 resistance vs J

Figure 4.8 shows the resistance vs short circuit current density.

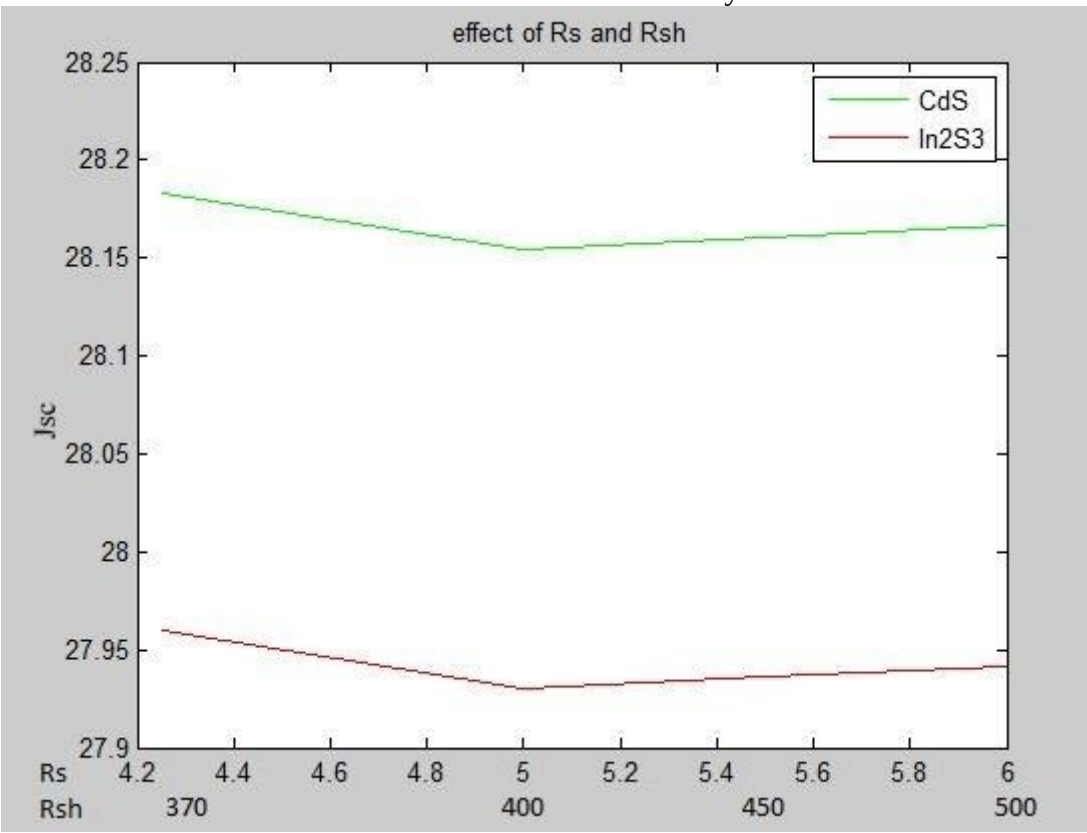

Fig 4.8 effect of resistances on J of solar cell

4.3.4 resistance vs V

Fig 4.9 shows the effect of resistance on solar cell

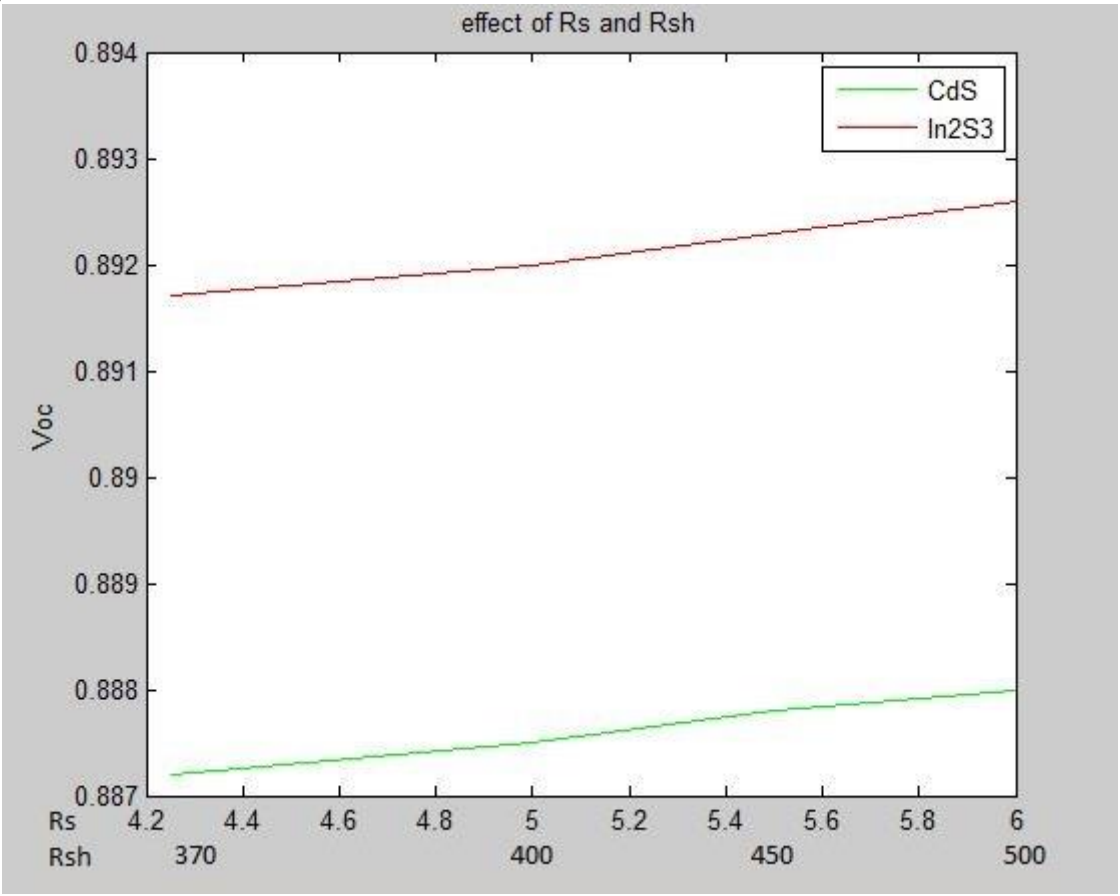

Fig 4.9 effect of resistances on V of solar cell

4.4 effect of thickness of absorber layer

Increasing the thickness of absorber layer increases the rate of photon incidence and absorption.

4.4.1 effect of thickness of CZTS layer on efficiency

Fig 4.10 shows the effect of thickness of CZTS layer on efficiency of solar cell

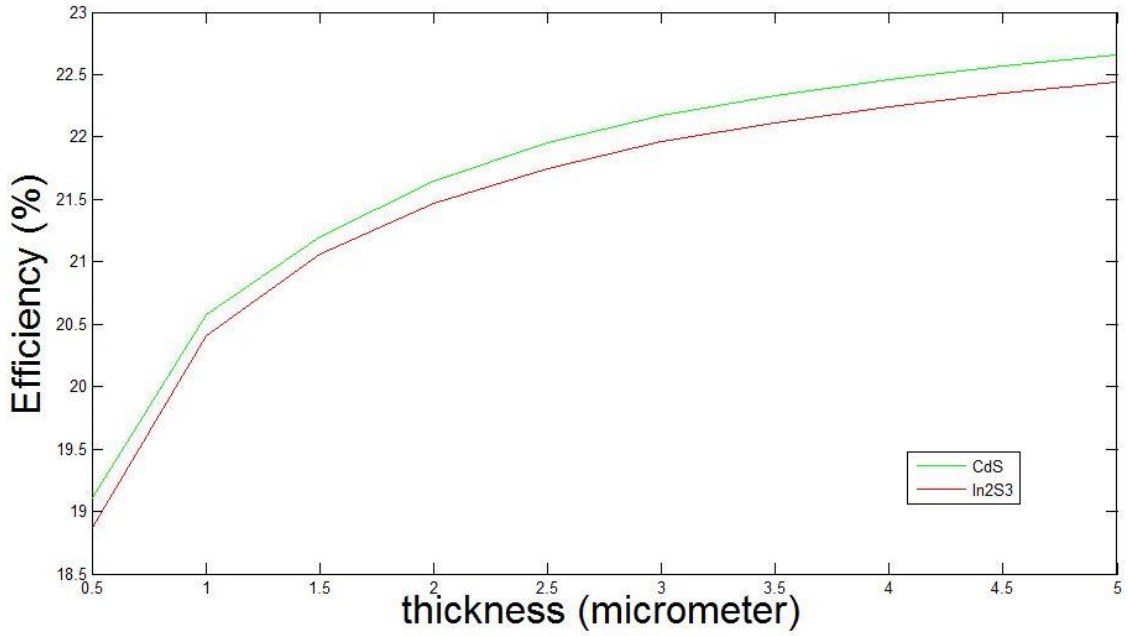

Fig 4.10 effect of thickness of CZTS layer on efficiency of solar cell

4.4.2 effect of thickness of CZTS layer on FF

Fig 4.11 shows the effect of thickness of CZTS layer on fill factor of solar cell

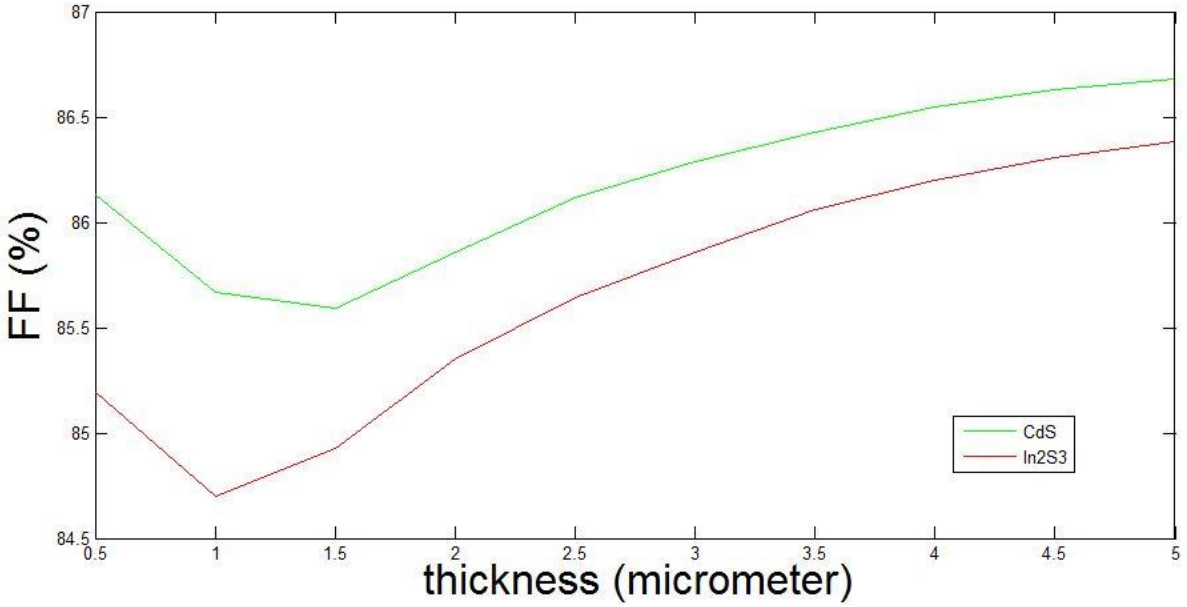

Fig 4.11 effect of thickness of CZTS layer on fill factor of solar cell

4.4.3 effect of thickness of CZTS layer on J

The effect of thickness of CZTS layer on short circuit current density of solar cellis shown in Fig 4.12

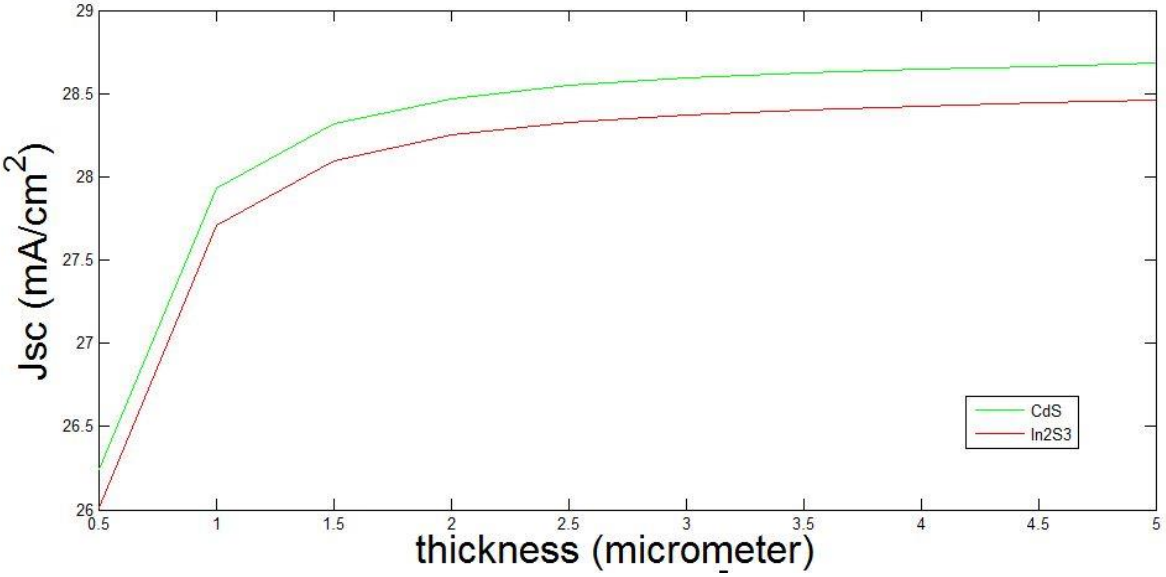

Fig 4.12 effect of thickness of CZTS layer on short circuit current density of solar cell

4.4.4 effect of thickness of CZTS layer on V

Fig 4.13 shows the effect of thickness of CZTS layer on open circuit voltage of solar cell

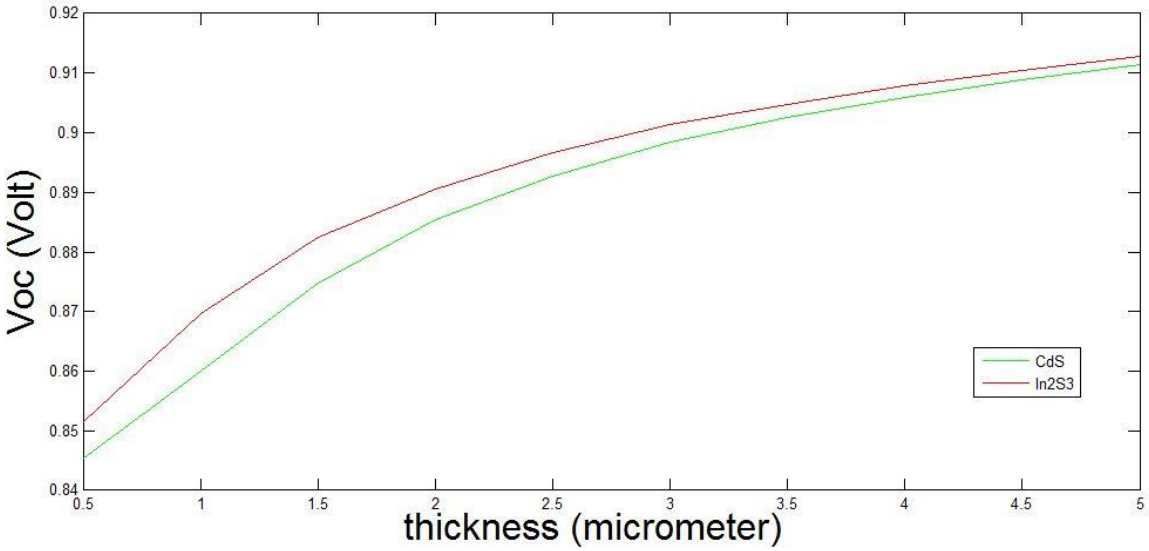

Fig 4.13 effect of thickness of CZTS layer on open circuit voltage of solar cell

4.5 effect of thickness of buffer layer

Increasing the thickness of buffer layer increases the rate of photon incidence and absorption.

4.5.1 effect of thickness of buffer layer on efficiency

Fig 4.15 shows effect of thickness of CZTS layer on efficiency of solar cell

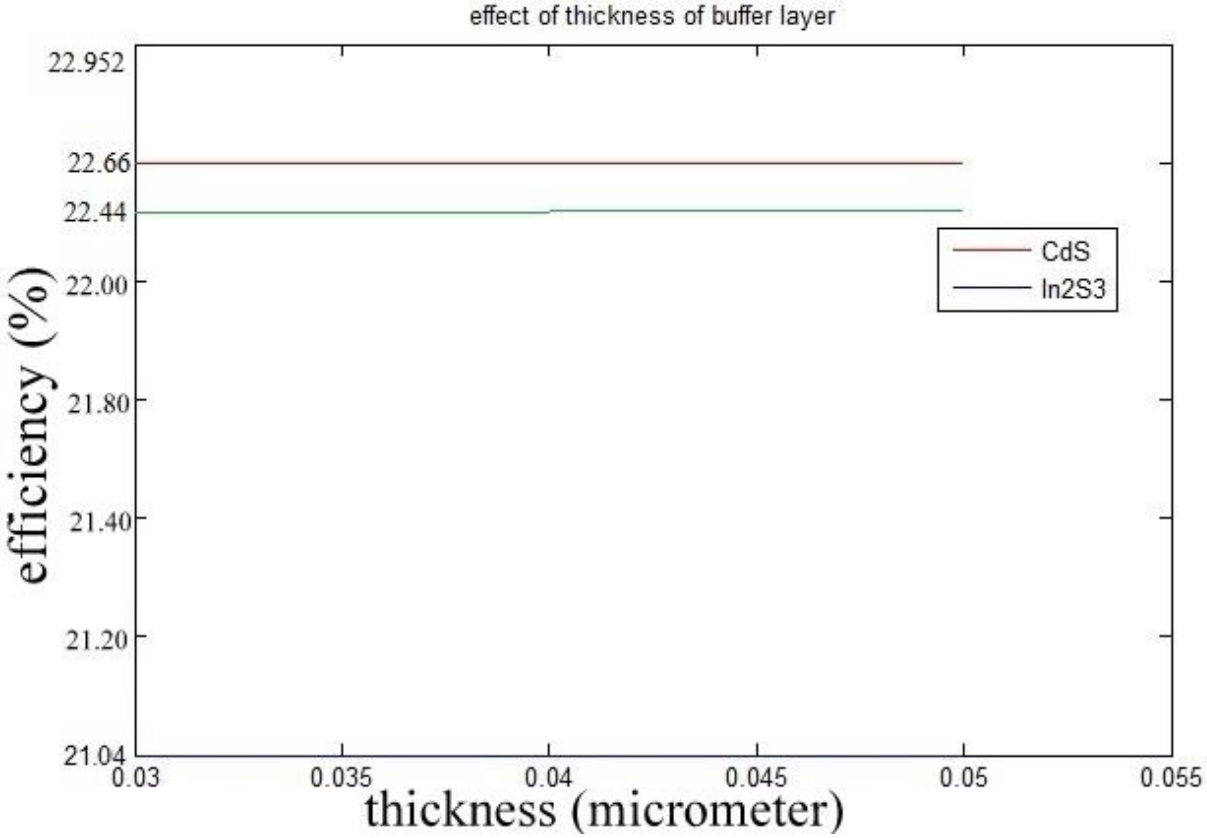

Fig 4.15 effect of thickness of CZTS layer on efficiency of solar cell

4.5.2 effect of thickness of buffer layer on FF

Fig 4.16 shows the effect of thickness of CZTS layer on fill factor of solar cell

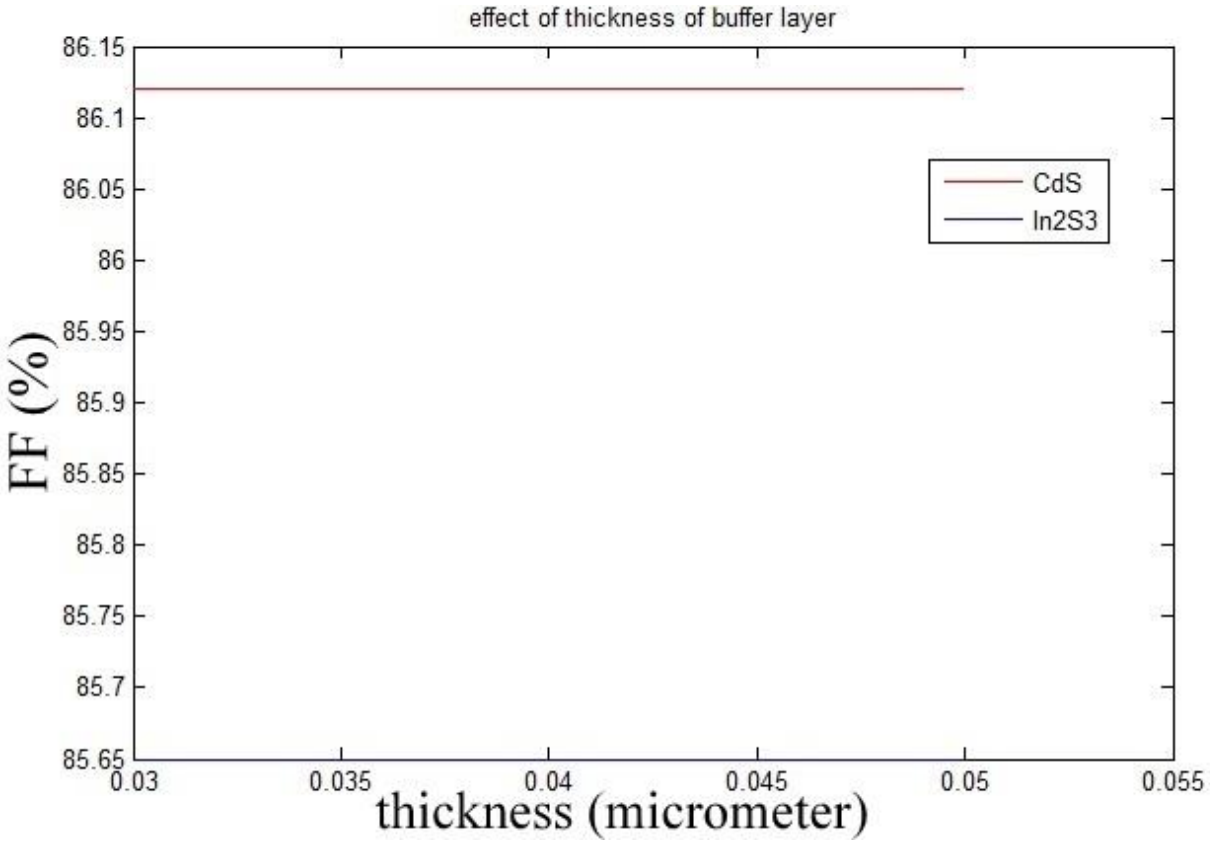

Fig 4.16 effect of thickness of CZTS layer on fill factor of solar cell

4.5.3 effect of thickness of buffer layer on J

Fig 4.17 shows the effect of thickness of CZTS layer on short circuit current density of solar cell

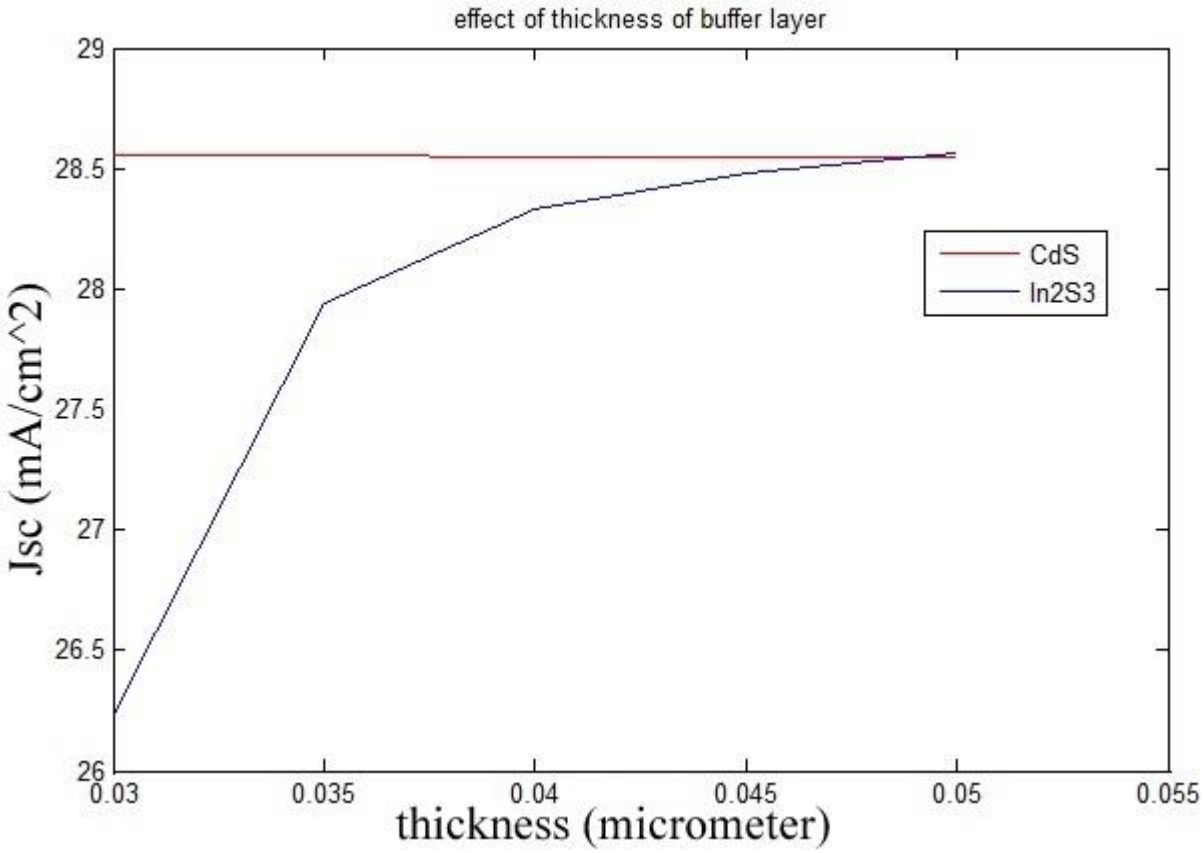

Fig 4.17 effect of thickness of CZTS layer on short circuit current density of solar cell

4.5.4 effect of thickness of buffer layer on V

Fig 4.18 shows effect of thickness of CZTS layer on open circuit voltage of solar cell

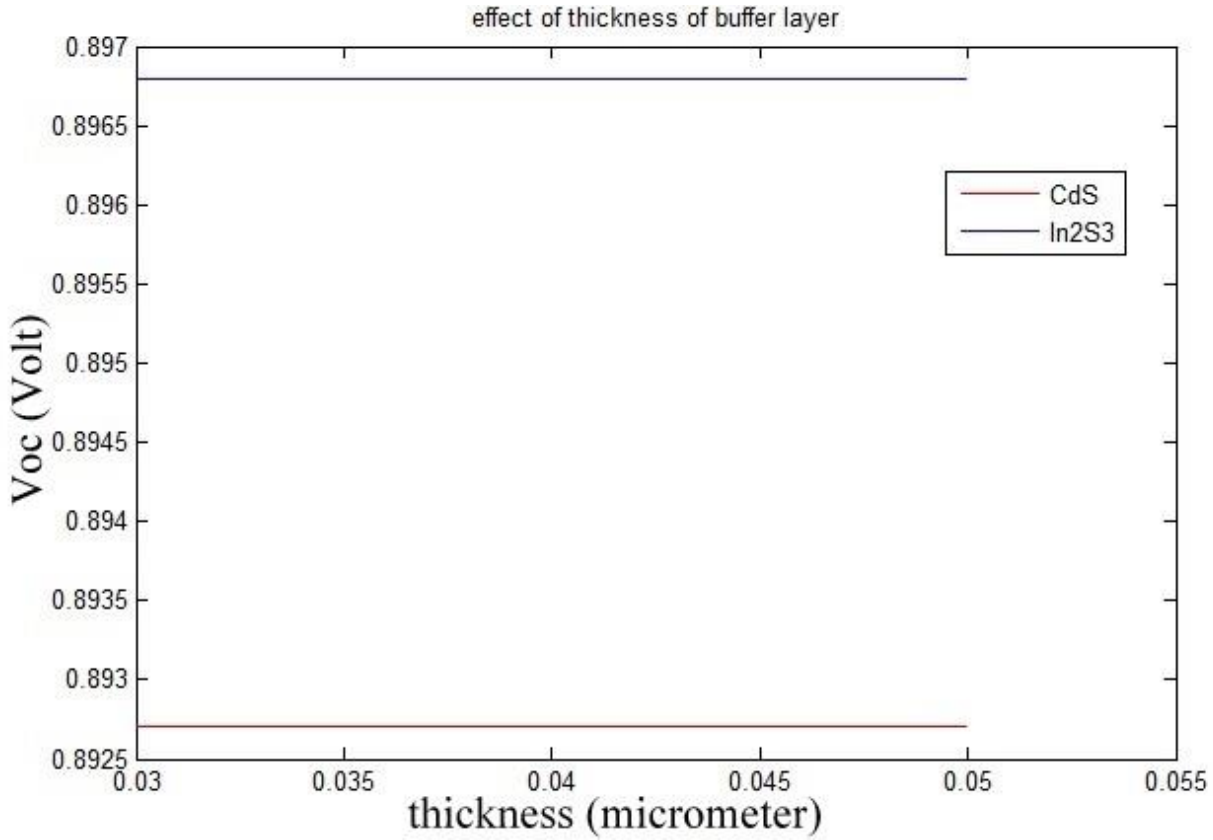

Fig 4.18 effect of thickness of CZTS layer on open circuit voltage of solar cell

4.6 effect of carrier density of absorber layer

4.6.1 effect of carrier density on efficiency

Fig 4.19 effect of acceptor density of CZTS layer on efficiency of solar cell

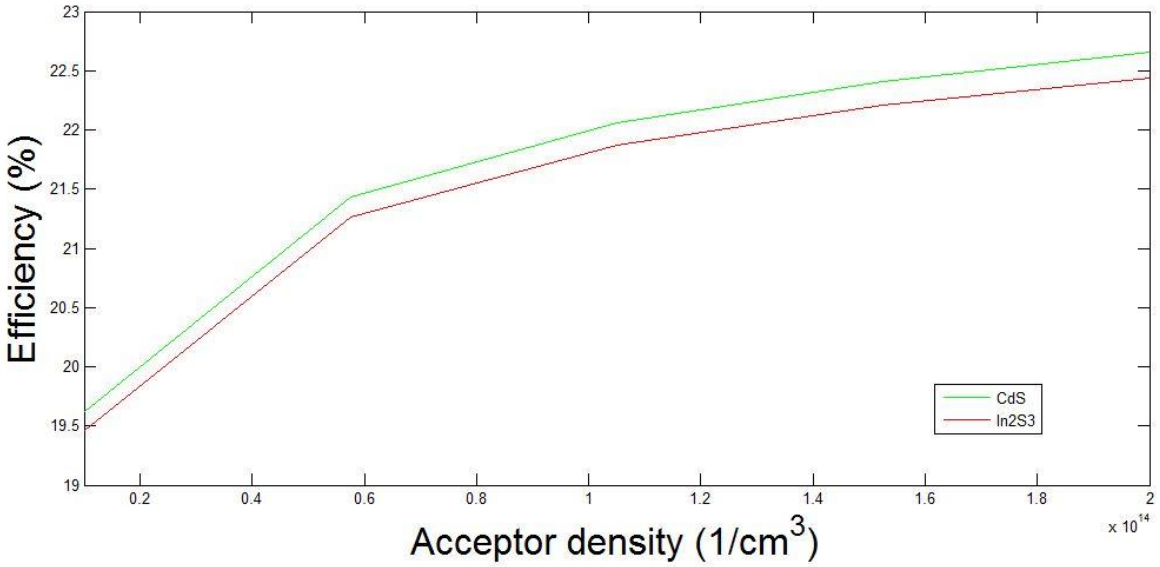

Fig 4.19 effect of acceptor density of CZTS layer on efficiency of solar cell

4.6.2 effect of carrier density on FF

Fig 4.20 shows effect of acceptor density of CZTS layer on fill factor of solar cell

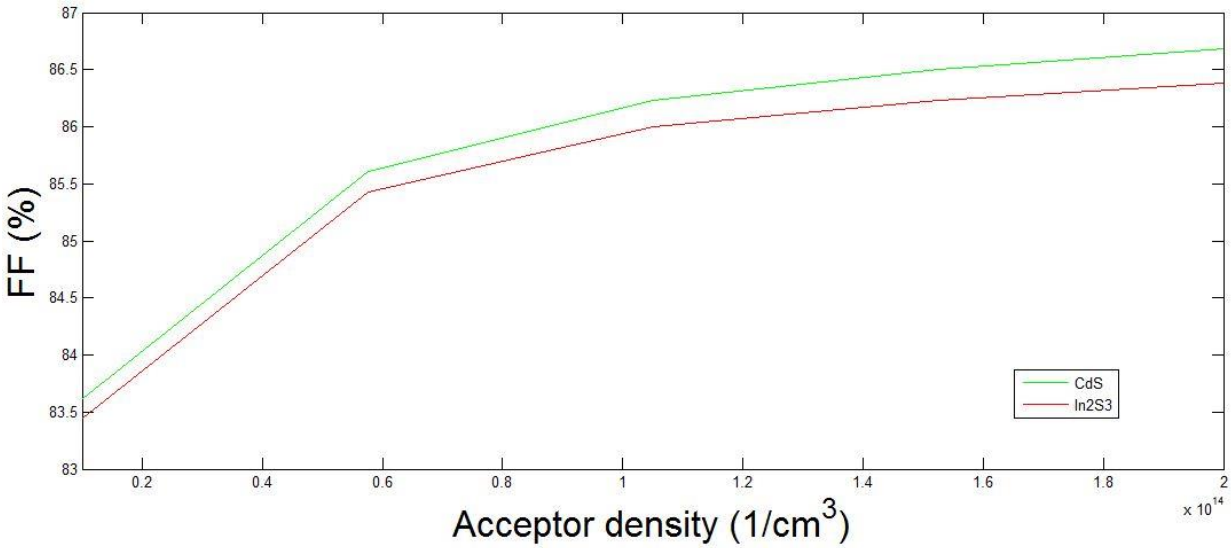

Fig 4.20 effect of acceptor density of CZTS layer on fill factor of solar cell

4.6.3 effect of carrier density on J

Fig 4.21 shows effect of acceptor density of CZTS layer on short circuit of solar cell

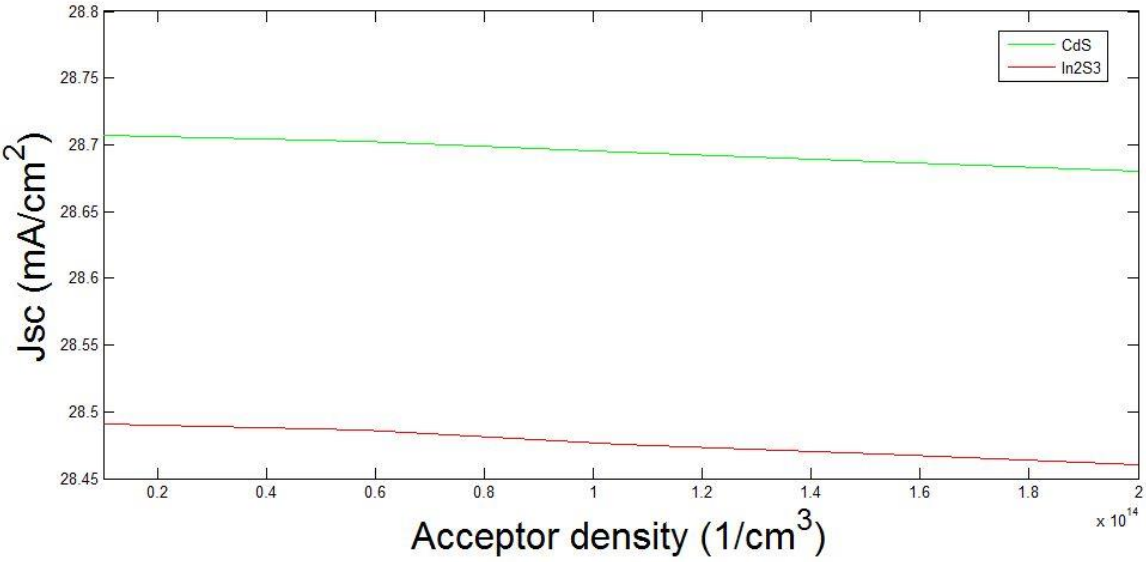

Fig 4.21 effect of acceptor density of CZTS layer on short circuit current density of solar cell

4.6.4 effect of carrier density on V

Fig 4.22 shows the effect of acceptor density of CZTS layer on open circuit voltage of solar cell

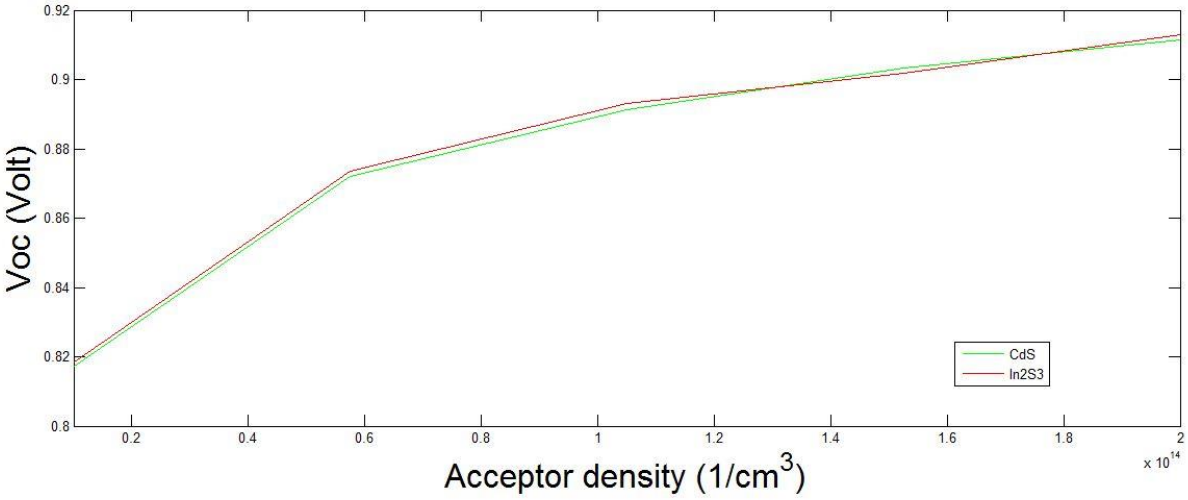

Fig 4.22 effect of acceptor density of CZTS layer on open circuit voltage of solar cell

5.1 Overview of the Work

In chapter 1, an overview of the research background, outline was presented.
This chapter was a gist of the thesis and research that went under in the course of it.

In chapter 2, the basic operational principles of solar cells, along with the basics of heterojunction solar cells were discussed. The application of II-VI compounds in solar cells, with an investigation into the high-cost issue of II-VI solar cells, which is the limiting factor for the mass fabrication of these solar cells were also discussed. CZTS solar cell was discussed and some major drawbacks of the CZTS solar cell were presented along with its ever increasing popularity. This served as a motivation for the thesis. A brief outline was given of this research with a discussion of the novelty in proposed device with appropriate references.

In chapter 3, the methodology of the research was described. An initial design of a CdS/CZTS
heterojunction solar cell was introduced which served as the starting point of the simulation. Then two modified structure were proposed and modelled. First modification was to the window layer and second modification was to the absorber layer in conjunction with the best window layer obtained from the first modification. Later, the final modified structure was subjected to a thorough investigation that was aimed to analyse the co dependence of cell performance to the layer thicknesses of the core layers and operating temperature.

In chapter 4, results and discussion was presented where a detailed analysis was performed for modified design in the solar cell. The modified window layer was analysed for different molar composition profiles for achieving high efficiency. A separate investigation was performed to find the change in a particular output parameter (efficiency, Voc, Jsc, FF) due to molar variation in window layer of the cell with analysis of the outcomes with proper explanation of the underlying physics. Investigation was also done to find the change in output characteristics of the device with varying alloy composition in the absorber layer for an optimum window layer molar fraction found in the last section. Analysis was done separately for each output parameters in order to understand the effects more appropriately. The outcomes have been discussed, and the way of optimization of alloy composition at different layers was illustrated. Finally, a high efficiency design was proposed at the end of the chapter. Chapter 4 also analyses this new design against different input design parameters such as thickness of window layer, absorber layer, temperature. This chapter discusses the critical issues of fabrication, and brings necessary modifications in the designs of chapter 3 accordingly

5.2 Future Work

In the simulation we varied the thickness of the CZTS absorber layer and the buffer layer for which we used CdS and In_2S_3 to get the best results. As we considered all cases as ideal so we didn't take the effect of material defect and the effect of series (R_S) and shunt (R_{SH}) resistances into consideration. Because of that our simulations showed a high estimated efficiency of 22.66%. We chose CdS as buffer layer due to higher efficiency, 5 μm thick CZTS layer and acceptor density of CZTS as $2*10^{14}$ cm^{-3}. Although the practical efficiency of these type of solar cell isn't that high due to the effect of many varying parameters. But the good news is as using CZTS for absorber layer is a particularly new concept so there's much room for development. The efficiency and the other output parameters depend on how the cell is fabricated. New types of fabrication processes are being discovered in order to increase the cell efficiency. In future new kind of fabrication technique will be discovered and make the conversion efficiency of CZTS based solar cells higher and hopefully this kind of cell will be a suitable alternative to CdTe or CIGS based solar cell.

References

[1] L. S. MA, "Limitations of 'Renewable' Energy," Electrical Sciences, 2012.

[2] S. Goldenberg, "The Guardian," UK, 8 June 2015. [Online]. Available: http://www.theguardian.com/world/2015/jun/08/g7-leaders-agree-phase-out-fossil-fuel-use-end-of-century.

[3]M. McGrath, "BBC news," UK, 2 November 2014. [Online]. Available: http://www.bbc.com/news/science-environment-29855884.

[4]C. Jamasmie, "mining.com," 8 June 2015. [Online]. Available: http://www.mining.com/g7-agrees-to-phase-out-fossil-fuels-by-end-of-the-century/.

[5]R. Noufi and K. Zweibel, "High-Efficiency CdTe and CIGS Thin-Film Solar Cells: Highlights and Challenges," in *IEEE*, Hawaii, 2006.

[6]P. Grana, "Renewable Energy World," 10 Novmber 2010. [Online]. Available: http://www.renewableenergyworld.com/ugc/blogs/2010/11/the-efficiency-race-how-to-cdte-and-cigs-stack-up.html.

[7]M. A. Green, K. Emery, Y. Hishikawa, W. Warta and E. D. Dunlop, "Solar cell efficiency tables," *Progress in Photovoltaics: Research and Applications*, 2012.

[8]M. A. Green, K. Emery, Y. Hishikawa, W. Wartha and E. D. Dunlop, "Solar cell efficiency tables (Version 45)," *Progress in Photovoltaics*, p. 9, 2014.

[9]R. Niderost, "Empa materials sscience and technology," REMIGIUS NIDERÖST, 18 January 2013. [Online]. Available: https://www.empa.ch/web/s604/weltrekord.

[10]C. Zhang, J. Zhong and Z. Tang, "Cu2ZnSn(S,Se)4 thin film solar cells fabricated with benign," Higher Education Press and Springer-Verlag Berlin Heidelberg 2015, 2015.

[11]M. R. Ananthan and B. Mahalaksmi, "Review on CZTS based Solar Cells," *Advances in Natural and Applied Sciences*, 2014.

[12]P. S. Vasekar and T. P. Dhakal, "Thin Film Solar Cells Using Earth-Abundant Materials," in *Solar Cells - Research and Application Perspectives*.

[13]B. Shin, O. Gunawan, Y. Zhu, N. A. Bojarczuk, S. J. Chey and S. Guha, "Thin film solar cell with 8.4% power conversion efficiency using an earth-abundant Cu2ZnSnS4 absorber," IBM T. J. Watson Research Center, Yorktown Heights, NY 10598, USA, 2013.

[14]D. F. Sargent, R. Nitsche and P. Wild, "Crystal growth of quaternary 122464 chalcogenides by iodine vapor transport," *Journal of Crystal Growth*, 1967.

[15]H. Katagiri, K. Jimbo, W. S. Maw, K. Oishi and M. Yamazaki , "Development of CZTS-based thin film solar cells," *Thin Solid Films*, 2009.

[16]K. Wang, O. Gunawan, T. Todorov, B. Shin and S. J. Chey, "Thermally evaporated CU2ZnSnS4

solar cells," *Applied Physics Letters*, 2010.

[17]M. S. Fan, J.-H. Chen, M.-H. Fan, C.-T. Li, K.-W. Cheng and K.-C. Ho, "Copper zinc tin sulfide as a catalytic material for counter electrodes in dye-sensitized solar cells," *Journal of Materials Chemistry A*, 2015.

[18]A. G. Kannan, T. E. Manjulavalli and J. Chandrasekaran, "Influence of Solvent on the Properties of CZTS Nanoparticles," in *8th International Conference on Materials for Advanced Technologies*, 2016.

[19]S. Das, K. C. Mandal and R. N. Bhattachariya, "Thermally evaporated Cu2ZnSnS4Cu2ZnSnS4 solar cells," in *Semiconductor materials for Solar Photovoltaic cells*, Springerx series in materials science, 2015, p. 279.

[20]J. Henry, K. Mohanraj and G. Sivakumar, "Electrical and optical properties of CZTS thin films prepared by SILAR method," *Journal of Asian Ceramic Societies*, vol. 4, no. 1, 2016.

[21]张. 军, "Simon Fraser University," [Online]. Available: http://www.siat.cas.cn/xscbw/xsqk/201109/W020110913360382232254.pdf.

[22]A. Khalkar, K.-S. Lim, S.-M. Yu, S. P. Patole and J.-B. Yoo, "Effect of Growth Parameters and Annealing Atmosphere on the Properties of Cu2ZnSnS4 Thin Films Deposited by Cosputtering," *International Journal of Photoenergy*, vol. 2013, p. 7, 2013.

[23]I. D. Olekseyuk, L. D. Gulay, I. V. Dydchuk, L. V. Piskach, O. V. Parasyuk and O. V. Marchuk, "Single crystal preparation and crystal structure of the Cu Zn/Cd,Hg/SnSe24compounds," *Journal of Alloys and Compounds*, 2002.